

# How causal perspectives can inform problems in computational neuroscience

Eric W. Bridgeford<sup>1,†</sup>, Brian Caffo<sup>2</sup>, Maya B. Mathur<sup>1,\*</sup>, Russell A. Poldrack<sup>1,\*</sup>.

**Abstract.** Over the past two decades, considerable strides have been made in advancing neuroscience techniques, yet the translation of these advancements into clinically relevant insights for human mental health remains a challenge. This review addresses a fundamental issue in neuroscience – attributing causality – and advocates for the development of robust causal frameworks. We systematically introduce the necessary definitions and concepts, emphasizing the implicit role of causal frameworks in neuroscience investigations. We illustrate how persistent challenges in neuroscience, such as batch effects and selection biases, can be conceptualized and approached using causal frameworks. Through theoretical development and real-world examples, we show how these causal perspectives highlight numerous shortcomings of existing data collection strategies and analytical approaches. We demonstrate how causal frameworks can inform both experimental design and analysis, particularly for observational studies where traditional randomization is infeasible. Using neuroimaging as a detailed case study, we explore the advantages, shortcomings, and implications for generalizability that these perspectives afford to existing and novel research paradigms. Together, we believe that this perspective offers a framework for conceptualizing, framing, and inspiring innovative approaches to problems in neuroscience.

**Introduction** Linear statistical models are a fundamental workhorse of neuroscience. Nearly every paper published in a neuroscience journal uses linear statistical methods such as analysis of variance (ANOVA) or regression modeling to estimate the strength of associations between variables and test statistical hypotheses regarding these associations. As an example of the prominence of these methods, a review of articles published in a recent issue of *Nature Neuroscience* (Volume 27 Issue 4, April 2024) found that 14 out of 15 of the articles presented results from ANOVA (12 articles) and/or regression modeling (8 articles).

One of the slogans that is taught in nearly every introductory statistical class is that “correlation does not imply causation.” Nonetheless, associations identified using linear statistical models (which encompass correlation) are almost always treated as if they reflect underlying causal mechanisms to some degree. This reflects the fact that the description of causal mechanisms is central to scientific explanation [1]; simply describing observed associations without interpretation would be of little interest to most scientists. The causal interpretation of statistical relationships is often reasonable in the context of experimental research, particularly when the treatment variables that have been randomly assigned, but in many cases inferences regarding causality are not supported by the data and model.

We propose that neuroscience needs to incorporate the insights that have been developed over the last three decades within the field of causal inference, many of which have been leveraged sparingly by neuroscientists in practice [2]. The tools developed by this field provide a basis for understanding when causal effects can be legitimately inferred from either experimental or observational data, and also provide a set of tools to understand the cases in which statistical models can result in biased inferences regarding causal mechanisms and to allow limited causal inference from nonexperimental data in some cases. A fundamental insight of this research is that the valid interpretation of any statistical model relies upon an understanding of the causal relations between the variables in the model as well as other variables not included in the model, **even if the goal is not to develop an explicitly causal or mechanistic model**. In the present paper we will provide an overview of the concepts and tools of causal inference that are relevant to understanding the validity of statistical estimates and inferences and demonstrate how they can provide new insights into common analytic situations that occur in neuroscience. We focus on the field of neuroimaging, given its important role in human neuroscience, but most of our conclusions are widely applicable across many areas of neuroscience.

<sup>1</sup> Stanford University, <sup>2</sup> Johns Hopkins University, \* these authors share senior authorship, † Corresponding author: Eric W. Bridgeford ([ericwb@stanford.edu](mailto:ericwb@stanford.edu)).

## 1 Identifying variables and estimands of interest

*Working Example 1: Neurofeedback for treatment of depression* In neuroimaging, researchers believe that brain activation patterns can be associated with mental illnesses, including depression [3]. Functional magnetic resonance imaging (fMRI) has been used alongside “neurofeedback” training, where people learn to achieve specific brain activation patterns. The goal is for individuals to access these patterns later, potentially reducing depressive symptoms. In causal inference, it is useful if the factor being studied can be experimentally manipulated in the real world<sup>1</sup> [5]. For example, the brain can be changed through medical procedures (like electrical stimulation), drugs, or psychological treatments (such as psychotherapy).

To illustrate this, researchers could study the effect of randomly assigning depressed individuals to either (1) neurofeedback training for anti-depressive brain patterns or (2) placebo training for unrelated brain patterns [6]. They would measure depression symptoms before and after treatment to see how much the symptoms changed. The difference in outcomes between the two groups (neurofeedback vs. placebo) would show the causal effect of the neurofeedback treatment.

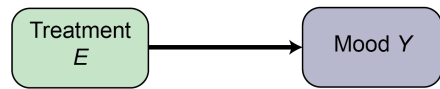
**1.1 The basics of causal inference and causal graphs** Causal inference typically begins by defining *variables* under study. Variables are used to summarize characteristics that will be analyzed, as well as extraneous factors that effect the characteristics that will be analyzed. In Figure 1(A), variables are denoted by boxes; the Treatment  $E$  would be the neurofeedback training administered, and the outcome  $Y$  denotes Mood. Causal relationships between these variables are denoted by arrows, which connect variables. Specifically, these arrows encode *causal mechanisms*. For a particular causal relationship, variable at the base of an edge is known as the *exposure*, and the variable at the head of the edge is typically known as the *outcome*. This requires that the outcome *occur temporally after* the exposure. For instance, if we were to administer neurofeedback training for anti-depressive activation patterns, we would anticipate that this may cause an individual’s mood to change, whereas changes in an individual’s mood would not cause them to be assigned to neurofeedback training. Across this review, there will typically be many variables and potential relationships between them; usually, an analysis will only focus on one of these relationships, known as the *estimand of interest*. An estimand of interest is a quantity of interest that one wishes to estimate, and is often related to an edge in the causal graph. For instance, one possible causal estimand of interest, the *average treatment effect*, represents the average effect that an exposure has on the outcome. This estimand is related to the edge  $E \rightarrow Y$  in the causal graph in Figure 1(A). We learn about this estimand through the *estimator*, which is a rule for computing a desired effect from the observed data.

*Identification of causal effects* The goal for causal analyses is to determine how the outcome would have changed between samples for a given intervention at exposure. For instance, in our working example, we may wish to clarify how mood changes if an individual were made to receive neurofeedback training versus if they were made to not receive neurofeedback training. On the other hand, a non-causal question may instead simply ask how the outcomes differ across naturally occurring exposure groups. The nuanced difference between causal and non-causal questions is that the former focus on the actual impact of the exposure itself, rather than just whether exposure and non-exposure groups differ. In non-experimental neuroscience studies, however, this is not directly estimable because other variables differ systematically by exposure groups. This means that conclusions can usually only be drawn about the impact of the exposure by generalizing across samples which receive different exposures. Causal inference is therefore concerned with *identification (ID) assumptions*: the assumptions under which conclusions about the causal effect of the exposure on the outcome can be drawn using the observed data. Stated another way, these define whether any estimator could validly estimate the

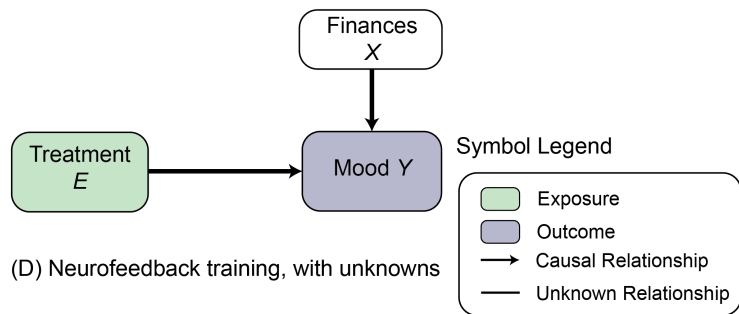
---

<sup>1</sup>While identifying causal effects without manipulability is more challenging, carefully-designed studies (such as audit studies [4]) can be employed to isolate causal effects while keeping other characteristics constant.

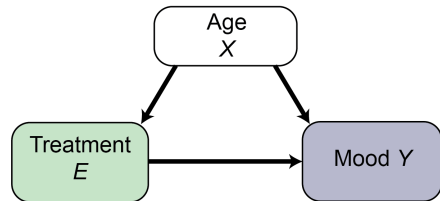
(A) Neurofeedback training RCT



(B) Neurofeedback training, with other variables



(C) Neurofeedback training, with common cause



(D) Neurofeedback training, with unknowns

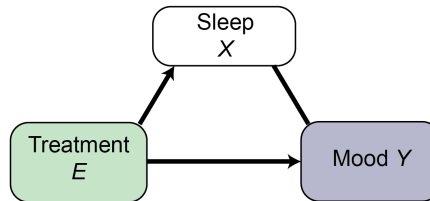


Figure 1: **Causal graphs illustrate assumptions about the underlying systems being investigated.** (A) A causal graph illustrating the depression-treatment example RCT. (B) A causal graph of the RCT, where there may be other variables that influence the outcome. (C) A causal graph where the exposure and outcomes are both altered by age. (D) a causal graph where the exposure affects sleep, but the relationship between sleep and mood is unknown.

causal effect of interest.

One of the more commonly used analytical techniques in neuroimaging is known as an *unadjusted bivariate analysis*: the process of deriving conclusions about the relationship between an exposure and an outcome by looking at how the outcome changes as a function of only the exposure, without analyzing other variables. Common examples include bivariate correlation analysis, linear regression, and analysis of variance (ANOVA); these analyses can be imprecisely referred to as “association”. These analysis methods make excellent candidates for exploratory analyses, as their application and interpretations often seem straightforward. In addition, they can provide evidence for causal relationships when certain data collection frameworks are utilized.

When we say that a technique provides evidence of a causal relationship, what we mean is the notion of *statistical consistency*; that is, if enough data were collected (and the technique involves sufficiently appropriate assumptions), relationships identified by the technique will correctly estimate the true underlying causal relationship. In scientific research, this effect is typically a causal estimand. Statistical consistency is closely related to (but distinct from) identification, in that identification specifically refers to whether (or not) the causal effect can be written as a function of the observed data. On the other hand, consistency refers to whether our specific chosen estimation technique (e.g., a regression) can recover this causal effect given infinite data. For instance, in the context of our experiment, identification would ask only whether it is theoretically possible (via any technique) to recover the effect of neurofeedback treatment on mood, whereas consistency would ask whether our chosen estimation technique (such as an ANOVA) would be able to recover the effect with enough data. Like identification, the consistency of estimators also typically rely on assumptions, which include the ID assumptions and additional factors. When the data do not meet one of these assumptions (ID or other assumptions) but we still attempt to draw causal conclusions, our conclusions can be biased. The *bias* of an estimator refers to its tendency to systematically mis-estimate an underlying effect.

**Randomized experiments** A *randomized experiment* (RE) is one where individuals are randomly assigned to exposure conditions; these are often also referred to as *randomized controlled trials* (RCTs). Imagine that there are other characteristics of our individuals which may have relationships with vari-

ables under study, such as financial stability. Financial stability may affect mood, which is denoted by the arrow from Finances to Mood in Figure 1(B). When data are collected under a randomized design, intuitively, the exposure assignment is typically not determined by any other variables. In Figure 1(B) this is denoted by the fact that there is no arrow from Finances nor Mood pointing towards the Treatment.

In other words, the exposure is *exogenous*; its value is imposed on the system by the assignment mechanism. Exogenous variables can be identified from causal graphs by identifying variables that do not have any arrows pointing into them; e.g., no variable points to treatment in the example above. This contrasts with *endogenous* variables, which are variables whose values may change in response to changes in other variables delineated by the system (e.g. mood may change when treatment changes). When the exposure is randomized across individuals, unadjusted bivariate analyses provide evidence of causal relationships with limited additional assumptions needed. In these situations, we would say that randomization of the exposure is a sufficient ID assumption for unadjusted bivariate analysis. In the neurofeedback example, an unadjusted bivariate analysis of mood (measured by depression scores) with treatment group is sufficient to derive causal conclusions. In fact, we could replace mood with a far more complicated outcome (such as a high-dimensional neuroimaging measurement, like a connectome), and conclusions drawn by simple unadjusted bivariate analyses would still be causal.

*The inadequacy of bivariate association in nonrandomized studies* Unadjusted bivariate analysis alone is often insufficient for deriving causal conclusions regarding direct effects of an exposure onto an outcome. For instance, consider the alternative setup in Figure 1(C). Consider that instead of randomizing individuals to the different neurofeedback treatments, the psychiatrists instead asked the individuals whether they wanted the targeted treatment or the placebo. If, for instance, younger participants were more willing to participate in the targeted treatment, and age were related to mood, age could jointly impact both the exposure and the outcome. Additionally, there may be other variables affected by the exposure with unknown relationships with the outcome under study. Consider that the targeted treatment could alter sleep, and the relationship between sleep and the outcome is unknown. These types of relationships are typically denoted with an undirected line, illustrated in Figure 1(D). In these cases and numerous others, detected variability from unadjusted bivariate analyses may be attributable to causal effects of the exposure on the outcome, or biases induced by failures to appropriately handle additional variables.

In this sense, the suitability of unadjusted bivariate analyses for deriving valid causal conclusions is often predicated on data collection mechanisms obeying the randomization (or similar) properties. When there are variables that have relationships with the exposure or the outcome which are changing non-randomly, unadjusted bivariate analyses can be insufficient for deriving conclusions that are consistent with the causal structure that generates the data. In these cases, bivariate analyses can be subject to biases that may yield spurious conclusions. This can materialize in a variety of ways, including erroneously detected effects (false positives), mistakenly non-detected effects (false negatives), and other ways that predictions/conclusions may not generalize outside of the specific study population collected.

**2 Identifying and controlling for confounding bias** As noted above, straightforward unadjusted bivariate frameworks are often insufficient when tackling issues in neuroscience. Outside of randomized designs and particular experimental setups, such as those discussed in Section 1, unadjusted bivariate frameworks can be subject to pernicious biases that drive false positives, false negatives, prediction biases, or other erroneous conclusions [7, 8]. In human neuroscience, we frequently deal with *observational data*, wherein experimenters lack explicit control over the exposure of interest. Unlike the experimental designs described in Section 1, not randomly assigning the exposure leaves open the possibility that exogeneity of the exposure cannot reasonably be assumed. Unfortunately, unadjusted bivariate procedures can be completely misleading analytical tools under these situations [9].

*Working example 2: Batch effects in mega-analyses* Consider a multi-site consortium study, where for each individual, we measure the connectome  $Y$ , know the measurement site, and have demographic information (such as Age or Biological Sex). In such studies, researchers typically aim for *mega-analyses*, which involve aggregating individual-level data across multiple sites to obtain a more extensive demographic representation than is feasible at a single site under similar experimental conditions [10]. The ultimate objective is to perform a pooled analysis to gain insights into the connectomes  $Y$  collectively, such as identifying the effect of Biological Sex on the Measurements (Figure 2(A)). A significant challenge arises in many scientific modalities due to what are known as batch effects, loosely defined as “systematic technical differences when samples are processed and measured in different batches and which are unrelated to any biological variation” [11]. In simpler terms, these are signatures or biases in the data linked to the approaches or characteristics of the data collection process, unrelated to genuine biological signals of interest in the data. In this sense, neuroimaging analyses mega-analyses typically feature the arrow  $\text{Batch} \rightarrow \text{Measurement}$  (the *batch effect*). These differences may be attributed to technical design parameters (such as scanner models, parameters, or protocols), or non-technical reasons (such as technician proficiency, variability between devices of the same model, etc.); the notion of “Batch” here captures both these technical or non-technical particularities.

In our study design, the relationship between batch assignment, demographics, and connectome data requires careful consideration. One might note that the inclusion or exclusion of different sites (batches) influences the demographic composition of our overall sample; e.g., it may be easy to assume that  $\text{Batch} \rightarrow \text{Age}$  or  $\text{Batch} \rightarrow \text{Biological Sex}$ , rather than the reverse. An individual’s demographics exist independently of and prior to any study recruitment; for instance, an individual may be measured in a batch as a result of proximity to a testing site, which is influenced by their demographics. Recruiting Batch A from a university area and Batch B from a retirement community would likely result in different age distributions between batches, but this does not imply that the Batch in which an individual is measured causes changes in individual demographics. Instead, demographics simultaneously influence both Batch and Connectome characteristics.

In a causal graph, we can determine causal relationships by following causal paths. *Causal paths* are alternating sequences of variables and relationships (indicated by arrows), where we can follow relationships from one variable to the next. For instance, a length-1 path could be denoted by the line from  $\text{Age} \rightarrow \text{Measurement}$  (a *direct effect* of the exposure on the outcome). A length-2 path could be denoted by  $\text{Age} \rightarrow \text{Batch} \rightarrow \text{Measurement}$  (an *indirect effect*). Variables upstream on a path (*ancestors*) are said to have causal relationships with variables downstream on a path (*descendants*).

Imagine, for instance, that we are interested in identifying how Age changes the Measured connectome (Figure 2(A)). In this example, we have bold-faced the arrow  $\text{Age} \Rightarrow \text{Measurement}$  to indicate our relationship of interest. We pool our two datasets of interest, which were collected from cohorts with disparate Age and Biological Sex distributions. Notice that we have two causal paths that lead from Age to the Measurement: we have the causal path of interest  $\text{Age} \rightarrow \text{Measurement}$ , and an indirect causal path,  $\text{Age} \rightarrow \text{Batch} \rightarrow \text{Measurement}$ . Some analytical techniques, such as unadjusted bivariate techniques, can detect *total effects*, the cumulative effect of all possible pathways through which the exposure could influence the outcome. This means that detected variability would be due to two sources: the direct effect of Age on the Measurement (which we want to learn about), and the indirect effect of Age on the Measurement via Batch. The direct effect of Age on the Measurements cannot be identified with unadjusted bivariate techniques.

To overcome this limitation, one option would be to conduct a multivariate analysis (described in further detail in Section 2.1), an analysis in which we would condition on the mediator (Batch), such as a multivariate regression. The direct effect of Age on the Measurements can be straightforwardly identified through such techniques. For causal models with greater complexity than our example with four variables, other approaches may be derived from *causal mediation analyses* [12] which are strategies that attempt to attribute effects of an exposure on an outcome to either direct effects or indirect effects



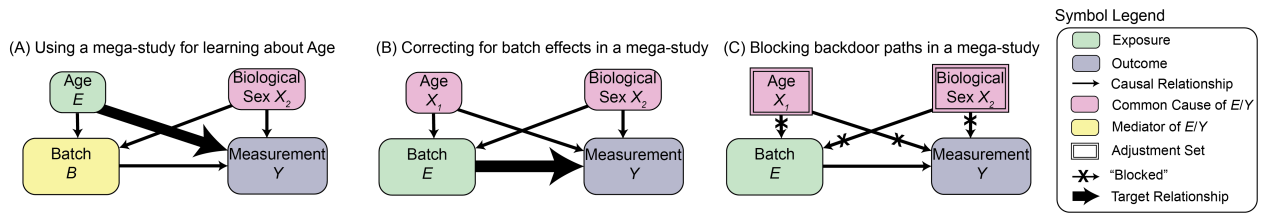


Figure 2: **(A)** a causal graph illustrating a typical mega-study analysis question, where we seek to learn about the relationship between Age and the Measured connectome. **(B)** the same causal graph as **(A)**, but where we seek to estimate the batch effect. Without adjustment for common causes, non-causal variability may exist between Batch and Measurement. **(C)** the same causal graph as **(B)**, using the observed covariates Age and Biological Sex as an adjustment set. Adjusting blocks backdoor paths (black Xs).

(e.g., those that work via mediators).

A common aim of mega-study is to collect a large dataset to approach many questions; for many such questions, the direct effect of a given covariate of interest on the Measurements would only be identified through conditioning on the Batch due to the “Batch Effect”, here denoted by the path Batch  $\rightarrow$  Measurement. To this end, neuroscientists instead typically attempt to “eliminate” this batch effect en-masse from the data via batch effect correction, through which investigators attempt to (implicitly or explicitly) estimate and remove the batch effect. Conceptually, this line of thinking goes, this “removes” the arrow Batch  $\rightarrow$  Measurement. If this arrow were no longer present, Batch would not be a mediator for addressing analytical questions such as those posed in Figure 2(A), and subsequent variability could, at least in theory, be ascribed to effects uncorrupted by indirect effects due to Batch. To this end, the remainder of this section will instead delineate approaches to understanding this batch effect (Figure 2 (B)). Notice that Batch is now the exposure of interest, because our analytical goal instead focuses on estimating and removing the batch effect.

**Backdoor paths and identification assumptions with additional variables** Isolating the effect of the Batch on the Measurement is a difficult problem due to backdoor paths. A *backdoor path* between an exposure and an outcome is a path that starts with an arrow pointing into the exposure and ends with a relationship pointing into or out of the outcome. For instance, in Figure 2(A), the sequence Batch  $\leftarrow$  Biological Sex  $\rightarrow$  Measurement denotes such a backdoor path. Recalling that arrows indicate a notion of “cause and effect”, Biological Sex is a common cause of the exposure and the measurement. A *common cause* (often also referred to as a *confounder*) is a variable that affects both the exposure and the outcome. When learning about the relationship between an exposure and an outcome, backdoor paths are nefarious. Troublingly, the changes imparted by common causes (if unsuitably addressed) can yield spurious relationships between the exposure and outcome, known as a *confounding bias*. For instance, if we were to compare measurements across batches using unadjusted bivariate analyses, these techniques would struggle to differentiate whether variability in the measurements was due to the different batches (the batch effect) or the age difference between participants (an Age effect). Unlike the randomized experiments of Section 1, the exposure is an endogenous variable.

Next, we consider the key ID assumptions with observational neuroscience data. Our working example is to identify how Measurements change due to the Batch (the batch effect). The first core assumption is known as *conditional ignorability* which states that we can account for all factors that affect both the exposures and the outcomes using only the observed covariates, and is also known as *no unmeasured confounding* [13, 14]. Violations of this ID assumption are the focus of Section 2.2. The second core assumption is known as *positivity*, which asserts that any given individual could plausibly have received either exposure level, based on their individual characteristics [15]. In the working example, this would mean that across all of the batches, there are no characteristics which could fully determine which batch someone were measured in. In observational studies, endogeneity issues often manifest through violations of the conditional ignorability and positivity assumptions. For instance,

if Batch A were only college-age students and Batch B were only geriatrics, we could hypothesize a violation of the positivity assumption, because Age determines Batch.

A third assumption, *exposure consistency*, focuses on the idea that each possible exposure corresponds to a single, well-defined intervention that could be obtained for a given individual (known as the *potential outcomes*), and that the exposure actually received corresponds to the potential outcome for that exposure level [16]<sup>2</sup>. For instance, in our previous example, if neurofeedback therapy were applied inconsistently over time to individuals, or different neurofeedback therapies were applied, this may pose a violation of exposure consistency. A fourth assumption, the *stable-unit treatment value assumption* (SUTVA), requires that exposed units are independent. Isolating the effectiveness of a vaccine may be difficult due to SUTVA violations, as a person receiving a vaccination affects the outcomes of others through herd immunity. It is important to clarify that all of the methods described herein assume the exposure consistency and SUTVA assumptions. Our below descriptions focus primarily on the conditional ignorability and positivity assumptions, because the methods described differ with regards to how they handle violations of these assumptions and how transparent they are under violations of these assumptions.

## 2.1 Conditional analyses and statistical consistency assumptions with additional variables

Taking steps to address confounding can be a simple and powerful way to increase confidence in subsequent conclusions. *Blocking all backdoor paths* is a process through which we identify a set of variables (an *adjustment set*, notated by square blocks in Figure 2(C)), and control for or stratify on these variables in analysis to control for confounding biases that can be imparted by these variables. If all common causes of the exposure and outcome are measured, these variables always form a valid adjustment set. Graphically, blocking paths eliminates causal paths between variables in the adjustment set and the exposure/outcome (Figure 2(C); note the black 'X's along backdoor paths). Statistically, backdoor paths being blocked by the adjustment set is equivalent to fulfillment of the conditional ignorability criterion by the adjustment set variables. After blocking, the variable that was previously a common cause can no longer transmit effects to both the exposure and the outcome (eliminating the confounding). This is the ultimate goal of “confound modeling” approaches in neuroscience, though they are rarely examined using a causal framework.

To gain intuition for some of these methods, we will consider a basic example where we have an outcome of interest (Measured connectomes), an exposure (Batch), and measured covariates which literature review suggest may be common causes (Age and Biological Sex). Our goal is to estimate the effect of the Batch on the Measurements, so that we can subsequently remove it. An expanded discussion of the specific methods discussed and their limitations is provided in Appendix A and Visontay et al. [2].

The most basic approach to analyzing observational data for causal inference is multivariate analysis, typically through multiple regression models [17]. An *outcome model* specifies how the outcome variable is influenced by the exposure (the treatment or intervention of interest) and covariates (other variables that might affect the outcome). For instance, in our working example, we would model the Measurements as a function of the Batch and the covariates (e.g., via a linear regression, such as ComBat [11, 18]). While these models can identify causal estimands when conditional ignorability and positivity assumptions are met, they make violations of key identification assumptions opaque. As noted by [19], if these violations are ignored, resulting analyses can be “useless for understanding phenomena... and [this criticism] is actually an understatement” [19]. Further, consistency of estimators of effects derived from multivariate methods rely heavily on the correctness of the specification of the outcome model, which is often unknown at the time of analysis. An expanded discussion of multivariate

---

<sup>2</sup>exposure consistency, a property of the exposure, should not be confused with statistical consistency, a property of an estimator for an estimand, defined in Section 1. Through the remainder of this section, “consistent” without a qualifier of “exposure” refers to statistical consistency.

analyses is provided in Appendix A.1.

To address some of these limitations, researchers often attempt to employ various techniques which can make more transparent certain types of violations of ID assumptions (typically, positivity). We will broadly refer to this class of methods as *positivity-aware methods*<sup>3</sup>. The most fundamental is *stratification*, where samples are divided into covariate bins (strata) and analyses are performed within each stratum [20, 21]. For instance, in the previous example, prior to performing our multivariate regression, we may first group individuals into sex-matched bins for a specified age range (e.g., one bin might be females between 10 and 20, and we might perform regressions of the Measurement onto Batch and Age for a given biological sex/age bin). This approach can offer enhanced robustness and make assumption violations transparent; for example, we may have evidence of a positivity violation if a given bin contains only individuals from one batch and not the other. However, it can suffer from dimensionality issues if the covariates are complicated and sensitivity to bin selection [22]. An expanded discussion of stratified analyses is provided in Appendix A.2.

*Re-weighted methods* offer another approach by changing the strength of each observation's contribution to the analysis, thus making observational studies more like randomized experiments [23]. These methods rely on the *propensity score* – the probability of receiving a particular exposure given the covariates. The *propensity score model*, typically fit using logistic regression or multinomial models, specifies how the exposure depends on covariates, and a fit propensity score model allows us to estimate these propensity scores. Key techniques include *propensity trimming* (PT), which removes samples with extreme propensity scores, and *inverse probability weighting* (IPW), which weights samples inversely to their propensity scores [24]. For instance, through inverse probability weighting, we would first estimate propensity scores using a logistic regression of the Batch onto Age and Sex, and then incorporate transformations of these propensity scores into a regression of the Measurements onto the Batch. Positivity violations are made transparent by these methods, as the propensity scores will be extremely high (or low) for certain samples when the exposure groups differ substantially. More sophisticated approaches include *doubly robust methods* like augmented IPW (AIPW) [25] or targeted maximum likelihood estimation (TMLE) [26], which can provide consistent estimates (estimates that converge to the true value as sample size increases) if either the propensity score model or outcome model is correctly specified. These methods would incorporate the propensity score weights into approaches similar to multivariate methods. An expanded discussion of propensity score methods is provided in Appendix A.3.1 and Appendix A.3.2.

*Matching methods* take a more direct approach by pairing samples from different exposure groups based on covariate similarity [27]. For instance, matching methods might identify a reference batch, and then for each individual in the reference batch, identify individuals from other batches with similar covariates to that individual [28], prior to a regression of the Measurements onto the Batch. These methods aim to achieve covariate balance, a condition where the joint covariate distributions are approximately equal across exposure groups [23]. In these cases, positivity violations are made transparent through failures to identify matches across the exposure groups due to dissimilarities in the covariates of individual samples. While matching strategies can effectively balance covariate distributions [29], they face challenges with high-dimensional data and require careful selection of *distance metrics* (mathematical measures of covariate similarity between samples). An expanded discussion of matching methods is provided in Appendix A.3.3.

A crucial limitation across all these methods is their reliance on measuring relevant common causes. The challenge of unobserved confounding (when unmeasured variables affect both exposure and outcome) remains significant, as these methods can only account for measured common causes. Multiple

---

<sup>3</sup>These methods are often improperly characterized as “causal methods” or “causal analyses”; positivity-aware methods still require additional ID assumptions to derive causal conclusions, and non-positivity-aware methods can still yield causal inferences. In particular, no method can directly verify from the data the conditional ignorability criterion, and therefore all methods require assumptions and domain expertise regarding the sufficiency of observed covariates for causal conclusions.



regression is straightforward but can mask assumption violations regarding positivity, in contrast to positivity-aware methods. Stratification and matching are intuitive, but can be challenging with high-dimensional covariates, and propensity score methods can effectively balance groups but are sensitive to propensity model specification. The choice of method often depends on the specific context and data structure at hand. An expanded discussion of the limitations of different methods is provided in Appendix A.3.4. The assumptions and limitations of different methods are summarized in Table 1.

Method Type	Identification Assumptions					Robust to Some Misspecification		Diminishes Sample Size	Covariate Curse of Dimensionality
	Consistency	SUTVA	Positivity	CI	Positivity-Aware	Propensity Model	Outcome Model		
Multiple Regression	✓	✓	✓	✓	✗	N/A	✗	✗	✗
Stratification (non-PS)	✓	✓	✓ within strata	✓ within strata	✓	N/A	✗ robust to some misspec.	✗	✓
Propensity Stratification	✓	✓	✓ within strata	✓ within strata	✓	✗	✗ robust to some misspec.	✗	✗
IPW	✓	✓	✓	✓	✓	✗	✓	✓ reduced effective sample size	✗
Doubly Robust	✓	✓	✓	✓	✓	✓ either prop. or outcome misspec.	✓ either prop. or outcome misspec.	✓ reduced effective sample size	✗
Propensity Matching	✓	✓	✓	✓	✓	✗	✓	✓ reduced effective sample size	✗
Distance Matching	✓	✓	✓	✓	✓	N/A	✓	✓	✓

**Key**

✓ Yes or required  
✗ No or not required  
N/A Not applicable  
Desirable  
Less desirable  
Undesirable

Table 1: A comparison of methods for estimating causal effects from observed data, across various dimensions, including the identification assumptions, robustness to certain forms of model misspecification, whether the method reduces the sample size, and whether the method experiences difficulty when the number of covariates or common causes for the adjustment set grows. This chart summarizes the methods described in Section 2.1. Note that this chart is for conceptual purposes, and does not reflect every dimension of nuance for each technique.

*Potential for confounding in neuroimaging mega-studies* To illustrate the potential for confounding in neuroimaging mega-studies, we investigate demographic disparities (across site) in the Adolescent Brain Cognitive Development (ABCD) dataset [30] in Figure 3. The ABCD dataset is a large multi-site consortium study from 21 imaging sites across the United States.  $n = 11,757$  feature baseline demographic annotation provided in the ABCD Community Collection, a community resource featuring cleaned demographic descriptors and pre-analyzed MRI data [31]. While steps were taken to harmonize data collection protocols across sites, sites used different imaging protocols, and efforts have shown that there are likely site effects in the subsequent imaging data [32]. Site effects are analogous to batch effects, where the batch is taken to be the site of data collection. As many of these demographic variables would likely be common causes (simultaneously influencing brain connectivity and probability of measurement at a given site), differences would suggest risk for violations of basic causal ID assumptions in estimating site effects for removal with standard multivariate techniques.

As discussed in Section 2.1, causal methods typically address ID assumptions by re-weighting data such that exposures (sites) are effectively uninformative of common causes (i.e., the reoriented dataset is “effectively” a randomized experiment). When data are sufficiently simple, such as Appendix Figure 8, this can be discerned by direct plots of the covariates or the propensities; with strong violations of conditional ignorability or positivity, the covariate distributions tend to not overlap (Appendix Figure 8.A). However, when we have many exposures (such as the ABCD study) and many covariates, it is often desirable to instead turn to summary statistics of covariates of interest. For binary covariates (right-handedness, parent-identified sex of child as male, parent-identified racial/ethnic backgrounds), we compute the the percent of samples (within-site) with the indicated covariate. For continuous or ordinal (non-binary) covariates (age, parental income, level of parental education, neurocognitive measure principal components), we compute the normalized mean as the average covariate value (within-site), normalized by the global difference between the 95<sup>th</sup> and 5<sup>th</sup> percentiles. Global means across all samples are indicated by the black +. For binary covariates, we then test whether there are marginal differences across sites using the Fisher-Freeman-Halton test, an extension of the Fisher’s exact test procedure to binary data with more than two groups (number of null replicates = 10,000) [33]; for continuous covariates, we use the Kruskal-Wallis test, a variation of a non-parametric  $K$ -way ANOVA [34]. Across all covariates except percent parent-identified biological sex as male, marginal demographic distributions differ across sites ( $\alpha = 0.05$  after Bonferroni-Holm correction [35]). Consider demographic variables, such as social and environmental factors relating to the household in which a child is raised.

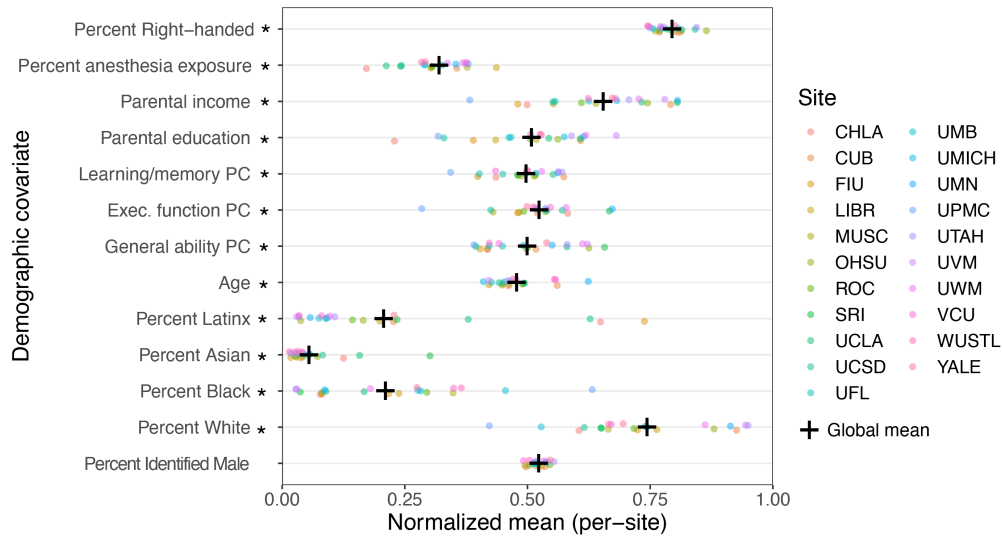


Figure 3: **Demographic disparities in the ABCD study.** The  $y$ -axis denotes different demographic descriptors in the ABCD study. For continuous or ordinal covariates (Parental income, parental education, learning/memory PC, exec. function PC, general ability PC, age), the  $x$ -axis denotes the normalized mean of the corresponding demographic descriptor, from 0 ( $5^{th}$  percentile) to 1 ( $95^{th}$  percentile). For binary covariates (Percent right-handed, percent exposed to anesthesia, percent Latinx, percent Asian, percent Black, percent White, percent biological male), the  $x$ -axis denotes the percent of samples (within-site) with the corresponding covariate. Colored points indicate the normalized mean for each site for a given demographic descriptor. The sample mean (across all sites) is indicated (black +). An asterisk (\*) is indicated to the right of an indicated covariate if the data indicate that the covariate differs across sites. Appendix Table 2 provides  $p$ -values for all statistical tests.

It is likely the case that the environment in which a child is raised is directly influenced by parental income and parental education, and that this developmental environment plays a role in subsequent brain function. Without incorporating many of these and other factors into batch effect correction models, batch effects are not identifiable, as the conditional ignorability criterion is not met. This motivates potential that naive multivariate techniques may run into violations of key ID assumptions in estimating and removing batch effects, and subsequent analyses would be extremely sensitive to modeling specifics.

**2.2 Unobserved confounding and sensitivity analysis** Our assessment of confounding control procedures in Section 2.1 and the related simulations can be summarized succinctly: when common causes are observed, we can incorporate them into adjustment sets, and then use these adjustment sets with causal methods to increase transparency of ID assumption violations. Unfortunately, measuring all potential common causes is usually difficult, especially when the observational data has already been collected and no new covariates can be observed. This is prevalent in neuroscience, where we may often have a limited or restricted set of covariates and demographic covariates about the individuals under study. This can materialize as a violation of the conditional ignorability ID assumption, in that exposed and unexposed individuals may differ in ways which are not measured. With these types of violations of the conditional ignorability assumption, inference can be meaningless, as most modeling approaches leverage this ID assumption (e.g., multiple regressions, stratifications, and re-weighting methods, described above). However, when combined with reasonably well-understood covariates and domain expertise, these methods can still be robust to certain types of unobserved confounding, and the potential impact of unobserved confounding on any result can also be estimated.

In Figure 4(A), consider that we have an additional measured common cause (Neuroanatomy), and an unmeasured Biomarker<sup>4</sup>. In this case, the Biomarker may be an unobserved common cause (often,

<sup>4</sup>In our figures, we explicitly delineate unmeasured common causes, so the arrow between Batch and Measurement is uni-directional. In practice, however, these variables are often omitted from causal graphs. In these cases, it is often practical

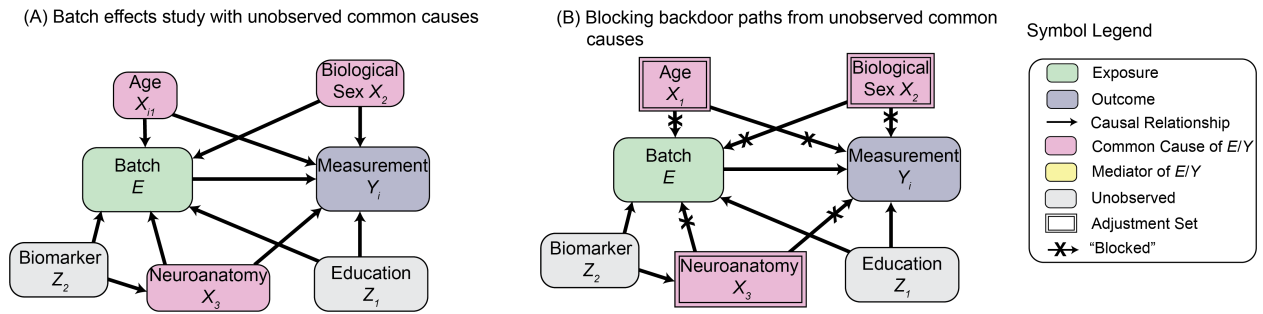


Figure 4: **(A)** the same causal graph as Figure 2(B), with an additional observed common cause (Neuroanatomy) and two unobserved common causes (Biomarker and Education). **(B)** including observed common causes in an adjustment set indirectly blocks the backdoor path through the Biomarker, but the backdoor path through Education remains open. Subsequent analytical attempts would be unable to rectify the causal effect of Batch on Measurement from the non-causal spurious variability due to the open backdoor path through Education.

genetic-related biomarkers will be unobserved in neuroimaging studies), because there is a potential causal path from the Biomarker to Batch, and a causal path from the Biomarker to the Outcome via Neuroanatomy. The potential backdoor path can be notated as  $\text{Batch} \leftarrow \text{Biomarker} \rightarrow \text{Neuroanatomy} \rightarrow \text{Measurement}$ .

Including Neuroanatomy in an adjustment set (e.g., via data pre-processing steps that correct for neuroanatomical differences) has the effect of blocking the backdoor path  $\text{Batch} \leftarrow \text{Neuroanatomy} \rightarrow \text{Measurement}$ , and also blocks the backdoor path  $\text{Batch} \leftarrow \text{Biomarker} \rightarrow \text{Neuroanatomy} \rightarrow \text{Measurement}$  (Figure 4(B), note the black 'X' from  $\text{Neuroanatomy} \rightarrow \text{Measurement}$  also blocks the path  $\text{Biomarker} \rightarrow \text{Neuroanatomy} \rightarrow \text{Measurement}$ ). The authors emphasize that this example is oversimplified, as it is likely there may be other ways in which genetics or underlying biomarkers could impact the exposure or the outcome other than just through Neuroanatomy. Further, it is unclear the extent to which “genetics” or “biomarker” represents a single coherent cause. There are many ways in which people can have genetic differences, and the impact of these differences on the connectome, or other variables may differ. That said, this example underscores the importance in practice of considering a causal graph, thinking about unobserved variables that might be present, and attempting to justify (via domain expertise and literature reviews) why potential backdoor paths might be blockable or not blockable in the system.

For an example of a potential unobserved common cause that cannot have its backdoor paths blocked using the observed covariates, consider Education in Figure 4(B). If one batch is collected at a university hospital and another batch is collected at a rural hospital, educational history may differ across batches, and also may impact the observed outcomes. We could also end up with an unobserved mediator effect similar to Figure 2(A-B), if one batch were collected in the morning, and another batch collected in the evening, and wakefulness mediated the relationship between Batch and Measurement, for similar reasons to those previously described in Section 2. This would result in the estimated batch effect also including variability due to the unobserved mediator. We illustrate the effects of unobserved confounding by augmenting our simulations to include an unobserved covariate in Appendix Figure 10. The implications of these results can be summarized intuitively: unobserved variables are problematic, insofar as they yield violations of the conditional ignorability ID assumption. When the unobserved variable is correlated with observed variables, we can still (partially) account for the unobserved factor using the observed variables (and therefore, conditional ignorability can still be satisfied). When unobserved variables are not correlated with observed variables, conclusions drawn from our analysis hinge on the degree to which this yields violations of the conditional ignorability assumption.

to denote when unknown or unmeasured common causes may be present to denote the relationship between an exposure and outcome with a bi-directional arrow.

From this simple example, it is clear that unobserved confounding can have an immediate consequence on our ability to derive causal conclusions, as the degree of correlation between observed and unobserved covariates is unknown in an observational setting. Uncertainty regarding unobserved variables has sparked skepticism about many groundbreaking discoveries; in one of the earliest debates of causal inference, the potential for an unknown gene that could cause both smoking and lung cancer was used by tobacco companies to undermine the discovery that smoking was associated with lung cancer [36, 37]. Much work in causal inference is dedicated to *sensitivity analyses* [38–41], which is “the study of how the uncertainty in the output of a model (numerical or otherwise) can be apportioned to different sources of uncertainty in the model input” [42, 43]. In causal inference, sensitivity analyses typically focus on “understanding the robustness of non-experimental findings [conclusions from observational studies] to a potential unobserved confounder [common cause]” [44]. Briefly, these approaches focus on the degree to which violations of the conditional ignorability ID assumption undermine the conclusions of the preceding analysis. Appendix C.2 details the use of one strategy for sensitivity analysis, known as the *E-value* [45], which assesses robustness of conclusions to unobserved confounding.

**3 Collision and Selection Bias** In Section 2, we introduced many approaches to “control” for confounding in analyses. These approaches “control” confounding by addressing endogeneity problems in the exposure. So far, we have discussed one type of confounding, *unobserved* confounding, where well-performing causal techniques could be subject to confounding biases when common causes were unobserved. When these unobserved common causes were, however, correlated with observed variables, control for the observed common causes may also partially or fully control for the unobserved common causes. Extending this intuition developed in Section 2.2 to its logical extreme, it may seem desirable to therefore measure and control for as many covariates as possible in an analysis, on the grounds that at least a subset of the observed covariates will probably correlate with unmeasured covariates. This logic is rather straightforward when all covariates can reasonably be assumed to be common causes; while increasing the number of covariates may result in fewer samples retained through matching or a lower effective sample size for propensity weighting techniques, bias of our conclusions will not generally be affected. There are, however, other types of variables that can be problematic, and controlling for these types of variables can actually introduce new biases to an analysis.

Consider professional football (soccer) players, where athletes are valued for their contributions to team performance. In football, different positions serve distinct roles: forwards and midfielders primarily score goals (offensive), while defenders and goalkeepers prevent them (defensive). A player’s proficiency in their primary role strongly influences their likelihood of reaching professional status, as teams construct lineups based on positional needs. This creates a causal structure where both offensive and defensive proficiency affect professional status, as illustrated in Figure 5(A). While these abilities are naturally unrelated, analyzing only professional players creates an apparent negative correlation between offensive and defensive skills. For instance, offensive players will tend to be selected in a sample of professional footballers almost entirely for being proficient at offense and almost irrespective of their defensive skill. This occurs because we have conditioned on professional status – a collider – leading to a biased subsample where players tend to excel in one area but not both, illustrated with the square box around professional status in Figure 5(B). In this case, professional status is known as a *collider* (or common outcome), in that it is a descendant of two variables (here, offensive and defensive skill). This artificially introduced *collider bias* resulting from conditioning on the collider (Figure 5(B), red dashed arrow) represents a common analytical challenge, particularly in neuroscience analyses.

In this case, the collider bias also introduces a *selection bias*, a bias which, loosely, occurs when the selection of individuals for analysis can bias subsequent conclusions.<sup>5</sup> Collider biases need not induce selection biases nor do selection biases imply the presence of colliders; however, these biases

---

<sup>5</sup>The phrase “selection bias” is typically used colloquially in statistical sciences; technically precise definitions of selection-related biases remain a subject of active inquiry [46, 47].

frequently co-occur in neuroimaging and population studies where samples are conditionally selected based on specific criteria, which is why they are useful for our illustrative purposes. To begin to understand selection biases, it is useful to define the concept of generalizability. Psychologists define internal generalizability as whether conclusions apply to the study population itself [48]<sup>6</sup>. External generalizability concerns whether findings extend beyond the study sample to other populations or the general population [48, 49]. A useful construction has been to therefore define the concept of internal and net-external biases.

In the simplest case when exposure does not affect selection, an internal bias occurs when estimates in the selected sample do not reflect true causal effects within that sample (threatening internal generalizability), while external bias occurs when causal effects in the sample do not match those in other populations (threatening external generalizability). However, when exposure affects selection, we need more precise definitions. An *internal bias* arises when conditioning on selection creates an artificial non-causal path between two variables [47]. For instance, in Figure 5(B), conditioning on professional footballers induces a misleading relationship between offensive and defensive skills. Net-external bias is a generalization of external bias that applies when the exposure affects selection. To understand net-external bias, consider how selection varies across groups: offensive skill heavily influences selection as a professional footballer for offensive players, but matters less for defensive players' professional status. A *net-external bias* is a bias which occurs when how outcomes would respond to an exposure differs across these groups of individuals whose membership in the selected sample can also be differently affected by the exposure [47].

*Working example 3: The problem of head motion* Head motion during neuroimaging data acquisition presents a two-fold problem. First, movement during an imaging session presents a spatial misalignment problem, in that areas (voxels) of an MRI that correspond to a particular area of neuroanatomy at one timepoint may not correspond to the same area of neuroanatomy at a sequential timepoint. This necessitates retrospective spatial realignment procedures, commonly referred to as *spatial motion correction* [50]. However, the impact of motion extends beyond spatial incongruence, inducing spatially heterogeneous signal perturbations that cannot be fully mitigated by realignment algorithms [51, 52]. These motion-induced signal fluctuations manifest as systematic measurement errors that are intrinsically linked to the neurophysiological signals of interest. In fMRI, these artifacts are particularly insidious, as they have been demonstrated to introduce spurious positive correlations in Blood-Oxygen Level Dependent (BOLD) time-series, potentially compromising functional connectivity analyses [51, 53]. The complex, non-linear nature of these artifacts poses significant challenges for their detection and correction, obfuscating true neurological dynamics from motion-related signal components.

Suppose we are attempting to characterize properties of the connectome related to brain-behavioral phenotypes, such as autism spectrum disorder (ASD) or attention-deficit hyperactivity disorder (ADHD). ASD and ADHD are known to be strongly associated with head motion issues in the confined environments of an MRI machine [54]. A causal graph for this experimental setup is illustrated in Figure 5(C); we have here illustrated the true underlying biological properties (which, conceptually, are captured by the measurements) that actually lead to behavioral phenotype changes and head motion issues. Here, head motion is also a collider of the exposure (Connectome) and the outcome of interest (the Behavioral Phenotype).

**3.1 “Addressing” head motion and selection biases** Addressing head motion for the case where the motion is subtle was an early goal of fMRI pre-processing [55], and many strategies have been developed in the decades since that continue to show promise [56, 57]. However, when this motion

---

<sup>6</sup>Many statisticians define this concept as internal validity; e.g., [46, 47]. However, in this work, we will make the distinction that generalizability is a statistical property (whether conclusions apply to a given population) and validity is a mechanistic property (whether a conclusion fully describes a desired mechanism), which is more analogous to its interpretation in the psychology and neuroscience literature.



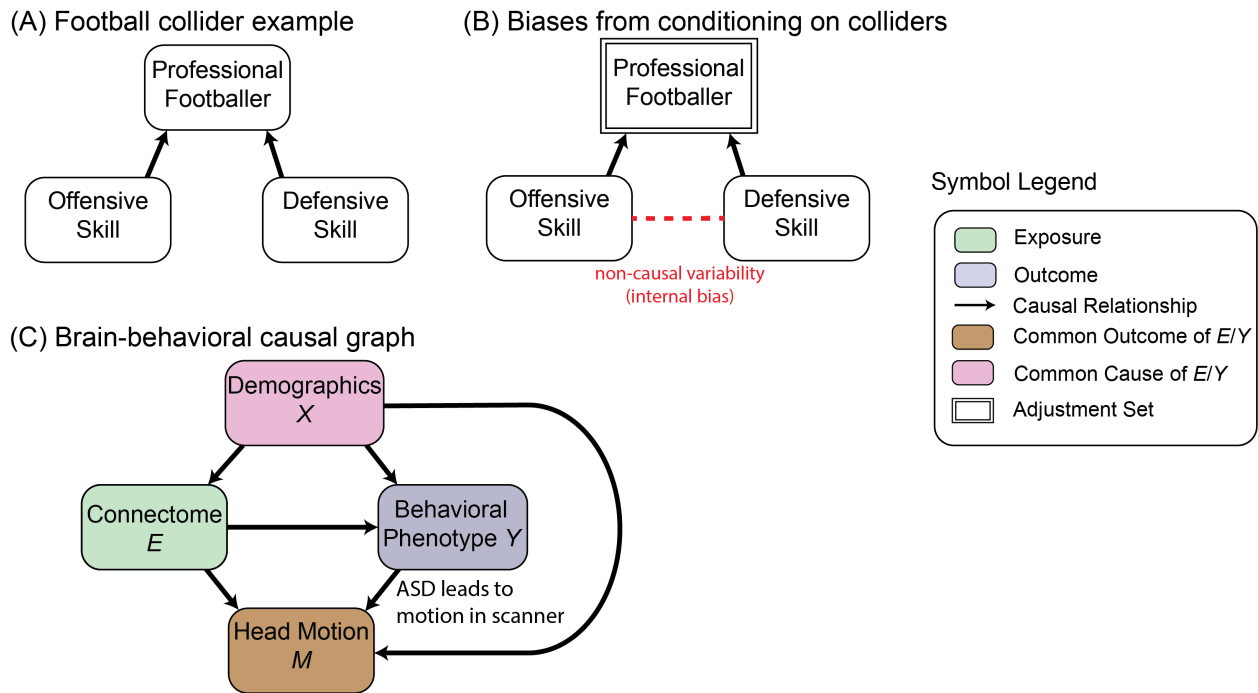


Figure 5: **Constructing appropriate causal graphs can be a crucial step to conducting appropriate inference.** (A) a causal graph depicting the football example, where status as a professional footballer is a common outcome (collider) of both offensive and defensive ability. (B) conditioning on professional footballers will identify spurious non-causal variability (delineated by the dashed edge  $---$ ) in the selected sample due to the internal bias. (C) a causal graph for a brain-behavior study. Note that head motion is a common outcome of both the connectome and the behavioral phenotype.

is substantial, many studies instead propose the outright exclusion of high-motion individuals [58–60]. In light of Section 2 and Figure 5(B), this has the effect of controlling for Head Motion via its inclusion in an adjustment set. However, Head Motion is a collider, and adjusting for it instead introduces new biases. In this case, restricting analysis to a subset of levels of a collider (such as excluding high-motion individuals) introduces a *collider stratification bias*, which is a bias that arises in an investigation due to conditioning an analysis on a collider. Conceptually, by controlling for Head Motion in this manner, we restrict ourselves to individuals with characteristics less predictive of head motion; for instance, those with less severe phenotypes for ASD/ADHD, or those with fewer predictive covariates for head motion [61]. This has the technical implication that it introduces non-causal relationships between the exposure and the outcome, limiting one’s ability to infer their true causal relationship even among those with less severe phenotypes for ASD/ADHD, much like conditioning on professional footballers could yield spurious variability between offensive and defensive ability. Non-causal approaches therefore provide three strategies, each of which are flawed:

1. Naive: Many post-processing approaches have been developed to address head motion [56, 57], but these approaches are only known to be reasonably effective for low-motion individuals [61]. Data from high-motion individuals likely remains corrupted with measurement errors, materializing as artificially high correlations in connectivity matrices [61]. Measurement errors are the focus of Section 4. The naive strategy simply analyzes the data as-is, and does nothing to address the collider nor the differential measurement error.
2. Filtering data within-individual: Some strategies, such as scrubbing, have shown promise for mitigating distortions due to high-motion timepoints by discarding high-motion timepoints all together [62]. If patient status affects motion, however, a causal lens reveals that these approaches selectively discard more data from patients than controls. Therefore, many of these solutions introduce new biases, in that (i) more signal is discarded (alongside the motion

artifacts) from patients than controls and creating a new differential measurement error, and (ii) one may introduce collider stratification biases in the temporal domain.

3. Filtering data at the individual level: High-motion individuals can be excluded entirely, introducing collider stratification bias. The `filtering` strategy removes individuals with high-motion.

Selection biases from filtering strategies have two distinct problems for generalizability. First, and more obviously, our conclusions may not generalize to the full population of interest since we’re analyzing only a biased subset of individuals (for example, those with lower head motion, who may have less severe ASD/ADHD symptoms). Second, and more subtly, our conclusions may not even be valid for this filtered subset itself. As shown by Mathur and Shpitser [47], selection-biased analyses can fail to produce reliable insights even when conclusions are restricted to the selected sub-population. This means that findings from motion-filtered neuroimaging studies of ASD/ADHD may be unreliable not only for the broader patient population, but also for the specific subset of patients whose data met inclusion criteria; that is, we face both internal and net-external biases (See [47], Table 2, Row B and the corresponding mathematical proofs for rigorous explanations).

*Selection biases in neuroimaging mega-studies* We investigate the potential for selection bias in the Adolescent Brain Cognitive Development (ABCD) dataset [30] in Figure 6. The Child Behavior Checklist (CBCL) is a screening checklist completed by parents which has shown promise as an aid for discerning the presence of potential ADHD symptoms in children [63]. This checklist provides a score designed to align with the Diagnostic and Statistical Manual of Mental Disorders (DSM) rating scale for ADHD, and can be used to construct tests with reasonable sensitivity for diagnosis of ADHD [64]. 11,236 children feature CBCL raw scores (Figure 6(A)). CBCL raw scores tend to correlate heavily with in-scanner motion. In-scanner motion is typically evaluated via the framewise displacement (FD), or the amount of motion from one frame of an MRI volume to the next. For each individual, the mean FD summarizes the average amount of motion (in mm) across all frames included in the baseline resting-state fMRI scanning session. We compute the average mean FD across individuals with a given CBCL raw score (Figure 6(B.I)). Individuals with lower CBCL scores tend to show lower FDs. This suggests that filtering approaches at the individual-level (e.g., excluding individuals entirely who have higher mean FD) will tend to disproportionately filter individuals more symptomatic of ADHD. A first-pass motion quality assurance for fMRI provided with the ABCD data is to assess the number of volumes that would be scrubbed with  $FD > 0.2$  mm. We show the average number of volumes retained after scrubbing volumes with  $FD > 0.2$  mm across individuals with a given CBCL raw score (Figure 6(B.II)). Individuals with lower CBCL scores tend to have more volumes retained after scrubbing. This suggests that filtering data approaches within-individuals will disproportionately discard more data from individuals more symptomatic of ADHD. This could yield the introduction of a collider bias through filtering approaches.

Colliders such as head motion can also introduce additional selection biases when they are common outcomes of variables other than just the exposure and outcome (e.g., Cosgrove et al. [65]). We apply a coarse inclusion/exclusion threshold for fMRI analyses, a mean FD exceeding 0.5 mm excluding data from subsequent analysis [62], and assess the characteristics of the resulting sample in Figure 6(C), using a similar approach to that described in Figure 3. For binary covariates, we test whether there are marginal differences across the groups of included and excluded individuals using the Fisher exact test [66]; for continuous covariates, we use the Mann-Whitney  $U$  (Wilcoxon rank-sum) test, a variation of a non-parametric 2-way ANOVA [67, 68]. Excluded samples by the criterion would tend to show higher CBCL raw scores (correlated with ADHD), have lower neurocognitive performance (learning/memory, executive function, and general ability PCs derived from neurocognitive tests), be younger, from traditionally underserved racial and economic backgrounds (Black, lower income, lower parental education), and would be more likely to be parent-identified as male ( $\alpha = 0.05$  after Bonferroni-Holm correction [35]). Subsequent analysis would therefore disproportionately exclude/include particular demographic groups, consistent with the conclusions from Cosgrove et al. [65]. The implications of these

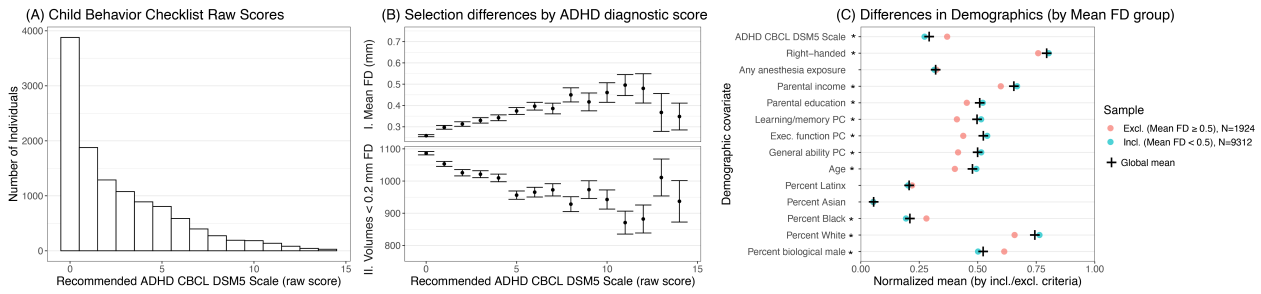


Figure 6: **Potential for internal and net-external biases in the ABCD study.** (A) the number of individuals from the ABCD study with an indicated CBCL raw score. For each raw CBCL score, the average (dot) and standard error (bars) across individuals (B.I) of the mean FD and (B.II) the number of volumes with  $< 0.2$  mm FD. (C) a plot analogous to Figure 3, where data are instead grouped based on whether the average mean FD exceeds 0.5 (exclusion for subsequent analysis) or less than 0.5 (inclusion for subsequent analysis). The sample mean (across all sites) is indicated (black +). An asterisk (\*) is indicated to the right of an indicated covariate if the data indicate that the covariate differs across groups. Appendix Table 3 provides  $p$ -values for all statistical tests.

characteristics on validity of the subsequent analysis is a focus of Section 4.2.

**3.2 Considerations for addressing head motions and selection biases** To address some of these shortcomings, Nebel et al. [61] note that despite the fact that individuals with ASD tend to move more and end up excluded, this is not always the case. That there are individuals whose demographic profiles would suggest a high likelihood for motion but have usable data may be exploitable for subsequent inference. With this observation in-mind, Nebel et al. [61] suggest excluding the individuals with high-motion, similar to `filtering`. After filtering, one can then retroactively re-weight the sample such that individuals who appear as though they should have high motion (i.e., they have the outcome or other covariates predictive of exclusion) but do not are factored more heavily into subsequent inference. This treats the motion correction problem as a missing data problem, where data from high-motion individuals is excluded and synthetically replaced with functions of data from lower motion individuals (albeit with similar predictors for high head motion). They develop the doubly robust targeted maximum likelihood (`drtmle`) strategy to proceed in this manner [61].

The phenomenon of reverse causation illustrates another potential pitfall in causal inference. A notable example is the 1981 study by MacMahon et al. [69] that found an association between increased coffee consumption (interpreted as the exposure) and pancreatic cancer (interpreted as the outcome). Initially, this led to the hypothesis that coffee consumption might cause pancreatic cancer. However, subsequent research revealed that early-stage pancreatic cancer often leads to digestive issues, prompting patients to reduce their intake of acidic beverages like coffee [70]. This case exemplifies *reverse causation*, where we investigate effects from the distribution of the exposure given the outcome, rather than the other way around. Subsequent conclusions may misattribute the true causal relationship (as in the erroneous case of coffee causing pancreatic cancer) or be uninformative for the underlying causal relationship entirely.

Brain-behavioral studies face similar challenges. Many of these studies examine associations between the exposure (the underlying biology via the measured connectome) and outcome in cross-sectional designs where the temporal ordering of variables remains unknown. Consider a simplified scenario: a healthy individual initially shows normal indicators for two arbitrary neurological biomarkers ( $x_1 = 0, x_2 = 0$ ). The true causal pathway might begin with subtle changes in one marker ( $x_1 = 1$ ) leading to diagnosable illness, after which both markers show more dramatic changes ( $x_1 = 2, x_2 = 1$ ). In a cross-sectional study observing only disease state, it becomes impossible to determine which connectome changes caused behavioral phenotypes or were downstream consequences of illness progression, as statistical analyses alone cannot adjudicate between these possibilities. Such approaches may target causal estimands, but these quantities are often not identifiable from the observed data

when the true causal direction is unknown or reversed. This leads to conclusions that can be artificial in nature rather than revealing true causal relationships, potentially confusing markers that caused disease progression with those that merely manifest as symptoms after diagnosis. It is crucial to recognize that the presence or absence of these non-causal effects does not necessarily imply the presence or absence of true causal effects, and vice versa. On the other hand, while modeling in a theoretically appropriate direction does not necessarily guarantee that causal relationships can be identified, researchers can at least delineate assumptions under which identification might be possible.

**4 Measurement error** The preceding examples illustrate how simplistic causal models reveal shortcomings in attempts to understand problems in human neuroscience. In particular, the latter two examples for batch effects and brain-behavior studies illustrate how attempts to rectify biases in the data itself can introduce challenges for subsequent analyses which are not obvious if not first passed through a causal lens. In both of these examples, the problems can be additionally characterized as *measurement error*, which occur when there is a difference between a measured value and the true underlying value of a phenomena one wishes to capture. While there may be errors in measurement of other properties, the primary problem of interest for both of these examples is the difficulty faithfully capturing a “stable” notion of brain connectivity; in the batch effects example, we anticipate that the site of measurement will impart site-specific biases to the measurements, and in the brain-behavior example, we anticipate that high amounts of head motion will lead to artificially inflated correlations in fMRI timeseries.

**4.1 Characterizing measurement errors** Measurement errors can be classified by their presentation. A *non-differential measurement error* is a measurement error in which conditional on adjustment covariates, both [71]:

- (i) the measured exposure is independent of the true outcome conditional on the true exposure, and
- (ii) the measured outcome is independent of the true exposure conditional on the true outcome.

To evaluate these examples, we will first consider the problem of estimating batch effects, in Figure 7(A). This Figure expands Figure 1(A) to include a separate variable for the true underlying connectome (denoted by  $Y$ ) and the measured connectome (denoted by  $Y^*$ ). Delineating a distinction between the true connectome and the measurement allows us to convey that Age and Biological Sex impact the Measurement through the Connectome, whereas the batch effect is captured by the direct effect of the Batch on the Measurement (which does not affect the Connectome itself). Here, the outcome of interest is the Connectome, and the exposure is the Batch. Conditioning on the Connectome and Age/Biological Sex would have the effect of blocking the backdoor paths of the form  $\text{Batch} \leftarrow \text{Age/Biological Sex} \rightarrow \text{Connectome} \rightarrow \text{Measurement}$ . However, the Measurement depends on the Batch in ways not captured by the true Connectome, which is via the path  $\text{Batch} \rightarrow \text{Measurement}$ . Therefore, this is a differential measurement error, because it does not satisfy condition (ii) in the definition of a non-differential measurement error.

We consider the problem of head motion in brain-behavior studies in Figure 7(B), which expands Figure 5(C). The Connectome (the true exposure  $E$ ) is a common cause of the Measurement (the measured exposure  $E^*$ ) and the Behavioral Phenotype (the outcome  $Y$ ). We have specified explicitly that the Connectome can impact Head Motion in ways other than just the Behavioral Phenotype of interest (e.g., ASD), such as via other behavioral phenotypes (e.g., those which materialize as symptoms of ADHD that are unrelated to ASD). Additionally, we have delineated the manner in which head motion corrupts our analysis; that is, that Head Motion alters the Measurements themselves via the path  $\text{Head Motion} \rightarrow \text{Measurement}$ . Conditioning on Connectome and Demographics would have the effect of blocking the backdoor path  $\text{Measurement} \leftarrow \text{Connectome} \rightarrow \text{Behavioral Phenotype}$ , similar to in Section 2. However, the outcome  $Y$  still influences the Measurement, via the path  $\text{Behavioral Phenotype} \rightarrow \text{Head Motion} \rightarrow \text{Measurement}$ . Therefore, this is a differential measurement error, because it does not satisfy condition (i) in the definition of a non-differential measurement error.

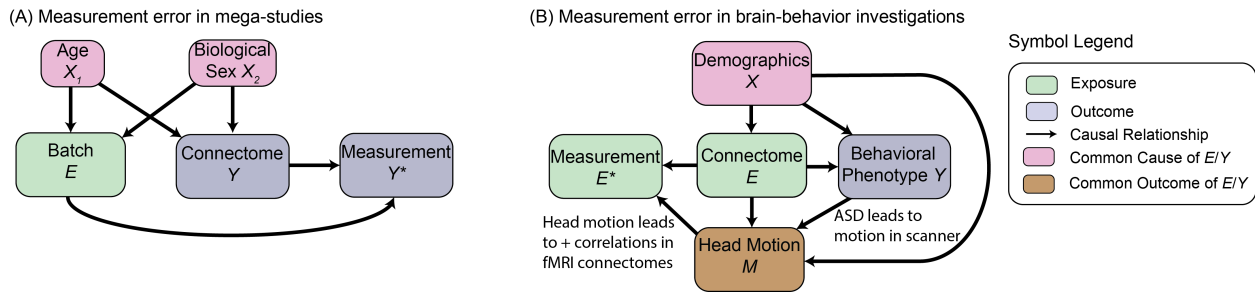


Figure 7: Plots illustrating differential measurement errors in **(A)** batch effects and **(B)** brain-behavioral studies, adapted from Figures 2(C) and Figure 5(C), by explicitly delineating the true underlying neurology (e.g., the Connectome) from its proxy Measurement (e.g., a connectome measured from fMRI).

**4.2 Considerations for measurement errors** It is routinely the case in neuroscience that many phenomena will imperfectly characterize the underlying property of interest. It is therefore common to omit the variable specifying the true underlying factor from the causal graph in certain situations. For instance, in Figure 7(A), one could omit the Connectome (as in Figure 2(C)), and all ancestral relationships for observed variables encoded by causal paths in Figure 7(A) are preserved: Age and Biological Sex are still ancestors of the Measurement, and the remaining causal paths are unchanged. It is important to clarify that subsequent assumptions would be with respect to the measurement, and not the true outcome of interest.

In other situations, omitting true underlying variables that are imperfectly measured yields non-identifiable causal estimands. For instance, consider omitting the Connectome in Figure 7(B). Here, the Connectome is a common cause for the relationships between the Measurement and the Behavioral Phenotype, Head Motion and the Measurement, and the Behavioral Phenotype with Head Motion. From Section 2.2, recall that unmeasured common causes of the exposure and the outcome yield violations of the conditional ignorability criterion. The implication is that no sufficient adjustment set exists using only the measured data; consequently, learning about the causal effect of the Connectome on the Behavioral Phenotype via the proxy Measurement directly via conditional procedures (e.g., multivariate methods, IPW, matching, etc.) is not possible, as a causal estimand is not identifiable. This means that no procedure could be proposed to identify causal effects in the context of the DAG in Figure 7(B), in light of both the differential measurement error as well as the potential selection bias issue due to the Head Motion collider (the focus of Section 3). Additional constraints and assumptions would need to be placed on the system to derive potential causal conclusions.

Using the model delineated in Figure 7(B), we investigate strategies one might use to investigate brain-behavioral relationships in Appendix C.3. Estimated effects tend to be uninterpretable, in that the estimates tend to be far from the underlying estimands, or the parameters one attempts to estimate. Further, while naive methods are sensitive to changes in effect size, the other techniques fail nominal sensitivity benchmarks, and none of the methods are particularly specific. We believe that these issues are likely due to a combination of not modeling the right relationships (e.g., reverse causation for `drtmle`), ignoring identifiability concerns due to the differential measurement error (e.g., naive), or introducing selection biases (e.g., filtering).

**Discussion** In this review, we outline how causal frameworks can be utilized to conceptualize and address challenges that arise in neuroscience. Our review has highlighted how traditional unadjusted bivariate analyses, while useful in certain contexts such as randomized experiments, are insufficient for addressing the complex issues inherent in observational studies where some variables of interest are not under experimental control. The pernicious biases that can arise in such studies and even extend into randomized experiments [47], including confounding and collider biases, underscore the need for more robust analytical approaches. Using causal graphs, we saw how these biases arise at the critical



stages of many neuroscience investigations, in the data collection itself, materializing as differential measurement errors. Analyses that account for confounding in principled ways, by directly addressing potential confounding, offer a potential path to more reliable conclusions. Our simulations demonstrate that these methods, particularly matching techniques, can greatly outperform traditional approaches when confounding is present, exchanging modest increases in variance due to decreases in sample size for far lower bias. Additionally, the challenge of unobserved confounding remains a critical issue, highlighting the importance of sensitivity analyses in assessing the robustness of causal conclusions.

*Implications for generalizability and validity* In Section 3, we defined the concepts of internal and external generalizability. In observational research, particularly neuroscience, confounding and other internal biases pose major threats to internal generalizability by potentially invalidating causal conclusions even for the observed data. Causal graphs, informed by domain expertise, serve as both visual and analytical tools for identifying these biases and clarifying the assumptions under which they might invalidate causal conclusions made on the basis of observed data. This approach guides researchers toward methods that explicitly consider (via identification assumptions) or address bias sources, contrasting with non-causal techniques that often require either randomized designs or unrealistic (or unsupported) modeling assumptions to support causal conclusions. Stated another way, causal inference facilitates transparent sets of assumptions (via ID and model specification assumptions) under which causal conclusions can be drawn from analyzed samples, which contrast from traditional analytical approaches.

Many researchers consider internal generalizability a prerequisite for external generalizability – findings should be valid for the study population before extending to different ones [49, 72]. While positivity-aware methods may offer stronger potential for external generalizability through their focus on bias reduction, they remain vulnerable to threats like unobserved confounding [49]. Further, while appropriate confounding control may facilitate reliable effect estimation in the selected sample, these effects may still fail to generalize to other populations via mechanisms such as net-external biases. Also, estimated average causal effects may not always match intuitive expectations about causality. An exposure could show opposing effects in different populations, with both results being statistically valid for their respective populations. This heterogeneity in exposure effects underscores the necessity of precisely specifying both population and context when discussing causal effects, particularly when selection processes might interact with exposure effectiveness.

In essence, causal methods may potentially forego broader samples for increased certainty within a narrower scope, analogous to exchanging an uncertain \$10 bill for a potentially more legitimate \$5 bill [73]. While this might reduce generalizability, it can enhance the reliability of conclusions within their specified domain. For example, techniques like propensity trimming and matching typically restrict the covariate range compared to the original data, due to their prioritization of causal identification in the analyzed data. This exemplifies the trade-off between internal and external generalizability: strengthening internal generalizability for a specific population may mean analyzing a more restricted sample, potentially limiting broader applicability. Further, the mechanisms through which samples are selected may introduce additional biases (e.g., internal or net-external biases via selection, as-per Section 3).

These concepts are closely related to the idea of internal validity, which in psychology is often conceptualized as whether an experiment can be used to delineate mechanisms for direct cause and effect relationships [74–76]. In many ways, generalizability can be thought of as a requisite to validity. Consider, for instance, an experiment where we seek to understand the mechanism underlying the link between a light switch and whether or not there is light in a room. We conduct an observational study, where we randomly flip light switches and observe whether the room lights up. Statistical notions of causality (e.g., ID assumptions and model specification assumptions) would identify a causal link, because randomly flipping light switches on causes light more often than not. Mechanistic notions of causality (e.g., depicted via a DAG of a circuit diagram) allow us to elucidate the assumptions under

which these conclusions relate to an actual mechanism (the circuit). Together, these notions provide us with tools (statistical approaches robust to the particularities of our data collection strategy) and a framework for interpretation (illustrated via the DAG) under which our inference is internally generalizable and valid with respect to an underlying mechanism. This creates a complementary relationship: internal generalizability (the assumptions of which are conveyed with ID and model specification assumptions) supports internal validity (the assumptions of which are encoded by the DAG), which in turn provides a foundation for external validity and broader generalizability. Understanding these relationships helps researchers make informed trade-offs between broad applicability and reliable causal inference.

*Future work* General works have focused on the difficulties of deriving causal inferences from human behavioral data [77], and several recent works have focused primarily on the limitations of neuroscience analytical techniques for yielding mechanistic causal conclusions from imaging data, due to the inherent complexities of brain function and the limitations of current neuroscience methods [78, 79]. We chiefly focus on the interplay between sampling schemes (e.g., via mega-analyses) and inclusion/exclusion criteria (e.g., filtering for head motion), and the manner in which these factors yield pernicious biases and errors in subsequent imaging (or more general) data. We believe that the insights we focus on here are complementary to these past works, and will become increasingly prevalent as the size, scale, and complexity of data collection consortia and data pre-processing and analysis efforts continue to grow. Siddiqi et al. [78] “propose a continuum along which to assess the relative strength of causal information”; we believe that understanding and developing techniques to appreciate the causal nature of measurement biases which arise or are introduced in these datasets represent a seminal hurdle along this spectrum sparsely addressed or properly framed as causal questions in the neuroscience literature. By addressing these foundational issues, we believe these efforts will strengthen the validity of inferences drawn from neuroimaging studies, ultimately advancing our understanding of brain structure and function and facilitating more specific subsequent mechanistic causal questions. As the field of neuroscience continues to evolve, integrating causal inference techniques and causal perspectives into standard practice will be crucial for advancing our understanding of brain-behavior relationships and translating neuroscience findings into clinically relevant insights.

*Recommendations for future neuroimaging mega-studies* Section 2 underscores the importance of methods for estimating and controlling batch effects. While we focus our efforts on the development of causally-informed methods for estimating batch effects, pre-hoc controls informed by causal perspectives can be implemented during data collection to limit the potential for confounding, obviating the need for causal methods entirely for this particular problem. This involves either randomizing measurement locations or explicitly controlling the study population to balance common causes across batches. Pre-experimental targets may include recruiting diverse cohorts across all batches or using modified case-control designs for pre-hoc covariate balance. Alternatively, a *crossed-over* design could be employed, measuring individuals across all batches while controlling participant state variables.

While full-scale implementation of these designs may prove infeasible, targeted study “arms” can serve as references for understanding batch effects. A “covariate-balanced arm” could identify demographically diverse subcohorts which are similar across sites, or a “crossover arm” could measure a diverse subcohort across all sites. These approaches may allow for direct study of batch effects with fewer limiting assumptions inherent in conditional approaches, potentially yielding generalizable causal batch effect control procedures that could then be applied to the broader study arm. This contrasts with existing conditional methods, where lack of covariate balance can lead to substantial confounding biases in batch effect estimation or correction. Care should be taken within this targeted arm to address potential mediating or confounding state variables, such as wakefulness.

*Recommendations for brain-behavior studies* Section 3 underscores the persistent challenge of selection bias, a well-documented issue in various domains of observational research [80, 81]. In brain-behavior studies using neuroimaging, this manifests prominently in the quantitative dissimilarity between data collected from specific behavioral phenotypes (e.g., ASD or ADHD) and typically-developing controls [61]. Through a causal lens, we saw that conditioning on head motion (via individual exclusion or specific censoring approaches like scrubbing) induces potential for both internal and net-external biases, and strategies ignoring head motion all together cannot identify causal effects from brain-behavioral studies. Our simulations illustrate that these and other creative approaches for estimating and testing effects in brain-behavioral settings lack both precision in estimation and robustness in testing performance. The suboptimal performance of these methods in controlled testing environments casts doubt on their validity for more complex inferential tasks and clinical utility. This conclusion presents a significant opportunity for advancement in neuroscience methodology.

The epidemiological literature offers a rich array of approaches for addressing measurement error, particularly in the realm of regression calibration, where estimates are “calibrated” to account for measurement errors [82]. While most extant methods address non-differential measurement errors, recent efforts have shown promise in developing techniques for differential measurement errors in controlled settings [83]. Although neuroimaging data presents unique challenges due to its high-dimensionality and continuous (rather than binary) exposures, these epidemiological approaches may serve as valuable theoretical foundations for future methodological innovations for mitigating the impact of motion-related noise artifacts from subsequent analyses. We posit that the development of causally-inspired methods holds the potential to substantially reduce bias in brain-behavior studies and pave seminal ground for clinical utility of neuroscience methodologies.

*Acknowledgments* This research was supported by the Noyce Foundation through the Women’s Brain Health Initiative Data Coordinating Center.

*Code and Data Availability Statement* Code and instructions for reproducing the figures and analyses contained within this manuscript can be found at [github.com/ebridge2/causal\\_neuro](https://github.com/ebridge2/causal_neuro). Real data exploratory analyses were conducted using data from the ABCD study [abcdstudy.org](https://abcdstudy.org), a longitudinal multi-site study designed to recruit and follow over 11,000 children into early adulthood. The data obtained for this manuscript were obtained via the NIH Neuroimaging Data Archive (NDA), a permissioned-access repository containing the ABCD study data. Access to this data requires an approved Data Use Certification (DUC), which can be obtained via NDA at [nda.nih.gov/abcd](https://nda.nih.gov/abcd). For more details on the data collection procedure, see Appendix D.

*Multiple comparisons considerations* Our real data exploratory analyses include numerous statistical tests ascertaining characteristics across different subsets of the ABCD study. To control the familywise error rate (probability of at least one type I error across all tests), we use Bonferroni-Holm correction across all  $p$ -values produced for analysis in Figures 3 and 6 [35].

*Inclusion and ethics* This study analyzed existing data from the ABCD study [30] accessed through the NIH Neuroimaging Data Archive under an approved Data Use Certification. The original data collection received appropriate IRB approvals with informed consent/assent from all participants and their guardians. Our exploratory analyses indicate that participants from traditionally underserved populations (Black participants, those with lower income and parental education) are disproportionately affected by common quality control procedures in neuroimaging, particularly motion-based exclusion criteria, supporting the results found by previous investigations (e.g., [65]). Our methodological recommendations aim to enhance inclusivity by identifying approaches that minimize systematic exclusion of underrepresented groups while maintaining scientific rigor. We emphasize that these issues represent both methodological and ethical imperatives, as biased participant selection directly impacts the equitable distribution of benefits from neuroscience research and may produce results that inade-

quately represent populations with behavioral phenotypes of interest such as ADHD symptoms. The causal inference frameworks we propose aim to make explicit the assumptions underlying neuroimaging analyses, thereby enhancing transparency and scientific integrity.

## References

1. William Bechtel and Adele Abrahamsen. Explanation: a mechanist alternative. Studies in History and Philosophy of Science Part C: Studies in History and Philosophy of Biological and Biomedical Sciences, 36(2):421–441, June 2005. ISSN 1369-8486. doi: 10.1016/j.shpsc.2005.03.010.
2. Rachel Visontay, Lindsay M. Squeglia, Matthew Sunderland, Emma K. Devine, Hollie Byrne, and Louise Mewton. Enhancing causal inference in population-based neuroimaging data in children and adolescents. Developmental Cognitive Neuroscience, 70:101465, December 2024. ISSN 1878-9293. doi: 10.1016/j.dcn.2024.101465.
3. Yvette I Sheline, Deanna M Barch, John M Donnelly, John M Ollinger, Abraham Z Snyder, and Mark A Mintun. Increased amygdala response to masked emotional faces in depressed subjects resolves with antidepressant treatment: an fmri study. Biological Psychiatry, 50(9):651–658, 2001. doi: 10.1016/S0006-3223(01)01263-X.
4. Corinne A Moss-Racusin, John F Dovidio, Victoria L Brescoll, Mark J Graham, and Jo Handelsman. Science faculty’s subtle gender biases favor male students. Proceedings of the National Academy of Sciences, 109(41):16474–16479, 2012.
5. Austin Bradford Hill. The Environment and Disease: Association or Causation? Proceedings of the Royal Society of Medicine, 58(5):295, May 1965. URL <https://www.ncbi.nlm.nih.gov/pmc/articles/PMC1898525>.
6. David M. A. Mehler, Moses O. Sokunbi, Isabelle Habes, Kali Barawi, Leena Subramanian, Maxence Range, John Evans, Kerenza Hood, Michael Lühns, Paul Keedwell, Rainer Goebel, and David E. J. Linden. Targeting the affective brain—a randomized controlled trial of real-time fMRI neurofeedback in patients with depression. Neuropsychopharmacology, 43:2578–2585, December 2018. ISSN 1740-634X. doi: 10.1038/s41386-018-0126-5.
7. Jody D. Ciolino, René H. Martin, Wenle Zhao, Edward C. Jauch, Michael D. Hill, and Yuko Y. Palesch. Covariate Imbalance and Adjustment for Logistic Regression Analysis of Clinical Trial Data. Journal of biopharmaceutical statistics, 23(6):1383, 2013. doi: 10.1080/10543406.2013.834912.
8. Robert A. Power, Julian Parkhill, and Tulio de Oliveira. Microbial genome-wide association studies: lessons from human GWAS. Nature Reviews Genetics, 18:41–50, January 2017. ISSN 1471-0064. doi: 10.1038/nrg.2016.132.
9. N. Gregory Mankiw. Macroeconomics. Worth, 8th ed edition. ISBN 978-1-4292-4002-4.
10. Joseph G. Eisenhauer. Meta-analysis and mega-analysis: A simple introduction. Teaching Statistics, 43(1):21–27, January 2021. ISSN 0141-982X. doi: 10.1111/test.12242.
11. W. Evan Johnson, Cheng Li, and Ariel Rabinovic. Adjusting batch effects in microarray expression data using empirical Bayes methods. Biostatistics, 8(1):118–127, Jan 2007. ISSN 1465-4644. doi: 10.1093/biostatistics/kxj037.
12. Kosuke Imai, Luke Keele, and Dustin Tingley. A general approach to causal mediation analysis. Psychological Methods, 15(4):309–334, December 2010. ISSN 1939-1463. doi: 10.1037/a0020761.
13. Paul R Rosenbaum and Donald B Rubin. The central role of the propensity score in observational studies for causal effects. Biometrika, 70(1):41–55, 1983.
14. Guido W. Imbens and Donald B. Rubin. Causal Inference for Statistics, Social, and Biomedical Sciences: An Introduction. Cambridge University Press, Cambridge, England, UK, April 2015. ISBN 978-0-52188588-1. doi: 10.1017/CBO9781139025751.
15. Donald B Rubin. Estimating causal effects of treatments in randomized and nonrandomized stud-

- ies. *Journal of Educational Psychology*, 66(5):688–701, 1974.
16. Stephen R Cole and Constantine E Frangakis. Consistency statement in causal inference: definition, identification and estimation. *Epidemiology*, 20(1):3–5, 2009.
  17. Alan Agresti. *Foundations of Linear and Generalized Linear Models (Wiley Series in Probability and Statistics)*. Wiley, Hoboken, NJ, USA, February 2015. ISBN 978-1-11873003-4. URL <https://www.amazon.com/Foundations-Linear-Generalized-Probability-Statistics/dp/1118730038>.
  18. Yuqing Zhang, Giovanni Parmigiani, and W. Evan Johnson. ComBat-seq: batch effect adjustment for RNA-seq count data. *NAR Genomics and Bioinformatics*, 2(3):lqaa078, September 2020. ISSN 2631-9268. doi: 10.1093/nargab/lqaa078.
  19. John Antonakis, Samuel Bendahan, Philippe Jacquart, and Rafael Lalive. *Causality and Endogeneity: Problems and Solutions*. OUP Academic, May 2014. doi: 10.1093/oxfordhb/9780199755615.013.007.
  20. P. Jepsen, S. P. Johnsen, M. W. Gillman, and H. T. Sørensen. Interpretation of observational studies. *Heart*, 90(8):956, August 2004. doi: 10.1136/hrt.2003.017269.
  21. Kenneth J. Rothman, Timothy L. Lash, and Sander Greenland. *Modern Epidemiology*. LWW, December 2012. ISBN 978-1-45119005-2. URL <https://www.amazon.com/Modern-Epidemiology-Kenneth-J-Rothman/dp/1451190050>.
  22. Andrew Gelman and Jennifer Hill. *Data Analysis Using Regression and Multilevel/Hierarchical Models*. Cambridge University Press, Cambridge, England, UK, December 2006. ISBN 978-0-51179094-2. doi: 10.1017/CBO9780511790942.
  23. Elizabeth A. Stuart. Matching methods for causal inference: A review and a look forward. *Statistical science : a review journal of the Institute of Mathematical Statistics*, 25(1):1, February 2010. doi: 10.1214/09-STS313.
  24. James Robins. A new approach to causal inference in mortality studies with a sustained exposure period—application to control of the healthy worker survivor effect. *Mathematical Modelling*, 7(9): 1393–1512, January 1986. ISSN 0270-0255. doi: 10.1016/0270-0255(86)90088-6.
  25. Heejung Bang and James M Robins. Doubly robust estimation in missing data and causal inference models. *Biometrics*, 61(4):962–973, 2005.
  26. Mark J van der Laan and Daniel Rubin. Targeted maximum likelihood learning. *The International Journal of Biostatistics*, 2(1), 2006.
  27. Elizabeth A. Stuart and Donald B. Rubin. *Best Practices in Quantitative Methods*. SAGE Publications, Inc., Thousand Oaks, CA, USA, 2008. ISBN 978-1-41299562-7. doi: 10.4135/9781412995627.
  28. Eric W. Bridgeford, Michael Powell, Gregory Kiar, Stephanie Noble, Jaewon Chung, Sambit Panda, Ross Lawrence, Ting Xu, Michael Milham, Brian Caffo, and Joshua T. Vogelstein. When no answer is better than a wrong answer: a causal perspective on batch effects. *bioRxiv*, page 2021.09.03.458920, February 2024. URL <https://doi.org/10.1101/2021.09.03.458920>.
  29. Daniel Ho, Kosuke Imai, Gary King, and Elizabeth A. Stuart. MatchIt: Nonparametric Preprocessing for Parametric Causal Inference. *Journal of Statistical Software*, 42:1–28, June 2011. ISSN 1548-7660. doi: 10.18637/jss.v042.i08.
  30. Nicole R. Karcher and Deanna M. Barch. The ABCD study: understanding the development of risk for mental and physical health outcomes. *Neuropsychopharmacology*, 46:131–142, January 2021. ISSN 1740-634X. doi: 10.1038/s41386-020-0736-6.
  31. Eric Feczko, Greg Conan, Scott Marek, Brenden Tervo-Clemmens, Michaela Cordova, Olivia Doyle, Eric Earl, Anders Perrone, Darrick Sturgeon, Rachel Klein, Gareth Harman, Dakota Kilamovich, Robert Hermsillo, Oscar Miranda-Dominguez, Azeez Adebimpe, Maxwell Bertolero, Matthew Cieslak, Sydney Covitz, Timothy Hendrickson, Anthony C. Juliano, Kathy Snider, Lucille A. Moore, Johnny Uriartel, Alice M. Graham, Finn Calabro, Monica D. Rosenberg, Kristina M. Rapuano, B. J. Casey, Richard Watts, Donald Hagler, Wesley K. Thompson, Thomas E. Nichols,



- Elizabeth Hoffman, Beatriz Luna, Hugh Garavan, Theodore D. Satterthwaite, Sarah Feldstein Ewing, Bonnie Nagel, Nico U. F. Dosenbach, and Damien A. Fair. Adolescent Brain Cognitive Development (ABCD) Community MRI Collection and Utilities. *bioRxiv*, page 2021.07.09.451638, July 2021. URL <https://doi.org/10.1101/2021.07.09.451638>.
32. Suheyra Cetin-Karayumak, Fan Zhang, Ryan Zurrin, Tashrif Billah, Leo Zekelman, Nikos Makris, Steve Pieper, Lauren J. O'Donnell, and Yogesh Rathi. Harmonized diffusion MRI data and white matter measures from the Adolescent Brain Cognitive Development Study. *Scientific Data*, 11(249):1–22, February 2024. ISSN 2052-4463. doi: 10.1038/s41597-024-03058-w.
  33. G.H. Freeman and J.H. Halton. Note on an exact treatment of contingency, goodness of fit and other problems of significance. *Biometrika*, 38(1/2):141–149, 1951.
  34. William H Kruskal and W Allen Wallis. Use of ranks in one-criterion variance analysis. *Journal of the American Statistical Association*, 47(260):583–621, 1952.
  35. Sture Holm. A simple sequentially rejective multiple test procedure. *Scandinavian Journal of Statistics*, 6(2):65–70, 1979.
  36. Ronald A. Fisher. Cancer and Smoking. *Nature*, 182:596, August 1958. ISSN 1476-4687. doi: 10.1038/182596a0.
  37. Jerome Cornfield, William Haenszel, E. Cuyler Hammond, Abraham M. Lilienfeld, Michael B. Shimkin, and Ernst L. Wynder. Smoking and Lung Cancer: Recent Evidence and a Discussion of Some Questions. *JNCI: Journal of the National Cancer Institute*, 22(1):173–203, January 1959. ISSN 0027-8874. doi: 10.1093/jnci/22.1.173.
  38. D. Y. Lin, B. M. Psaty, and R. A. Kronmal. Assessing the sensitivity of regression results to unmeasured confounders in observational studies. *Biometrics*, 54(3):948–963, September 1998. ISSN 0006-341X. URL <https://pubmed.ncbi.nlm.nih.gov/9750244>.
  39. James M. Robins, Andrea Rotnitzky, and Daniel O. Scharfstein. Sensitivity Analysis for Selection bias and unmeasured Confounding in missing Data and Causal inference models. In *Statistical Models in Epidemiology, the Environment, and Clinical Trials*, pages 1–94. Springer, New York, NY, New York, NY, USA, 2000. ISBN 978-1-4612-1284-3. doi: 10.1007/978-1-4612-1284-3\_1.
  40. H. Christopher Frey and Sumeet R. Patil. Identification and review of sensitivity analysis methods. *Risk Analysis : an Official Publication of the Society for Risk Analysis*, 22(3):553–578, June 2002. ISSN 0272-4332. URL <https://pubmed.ncbi.nlm.nih.gov/12088234>.
  41. Sander Greenland. Multiple-bias modelling for analysis of observational data. *Journal of the Royal Statistical Society: Series A (Statistics in Society)*, 168(2):267–306, March 2005. ISSN 0964-1998. doi: 10.1111/j.1467-985X.2004.00349.x.
  42. Andrea Saltelli. Sensitivity analysis for importance assessment. *Risk Analysis : an Official Publication of the Society for Risk Analysis*, 22(3):579–590, June 2002. ISSN 0272-4332. doi: 10.1111/0272-4332.00040.
  43. Andrea Saltelli, Ksenia Aleksankina, William Becker, Pamela Fennell, Federico Ferretti, Niels Holst, Sushan Li, and Qiongli Wu. Why so many published sensitivity analyses are false: A systematic review of sensitivity analysis practices. *Environmental Modelling & Software*, 114: 29–39, April 2019. ISSN 1364-8152. doi: 10.1016/j.envsoft.2019.01.012.
  44. Weiwei Liu, S. Janet Kuramoto, and Elizabeth A. Stuart. An Introduction to Sensitivity Analysis for Unobserved Confounding. *Prevention science : the official journal of the Society for Prevention Research*, 14(6):570, December 2013. doi: 10.1007/s11121-012-0339-5.
  45. Tyler J. VanderWeele and Peng Ding. Sensitivity Analysis in Observational Research: Introducing the E-Value. *Annals of Internal Medicine*, 167(4):268–274, August 2017. ISSN 1539-3704. doi: 10.7326/M16-2607.
  46. Haidong Lu, Stephen R. Cole, Chanelle J. Howe, and Daniel Westreich. Toward a Clearer Definition of Selection Bias When Estimating Causal Effects. *Epidemiology (Cambridge, Mass.)*, 33(5):

- 699–706, September 2022. ISSN 1531-5487. doi: 10.1097/EDE.0000000000001516.
47. Maya B. Mathur and Ilya Shpitser. Simple graphical rules for assessing selection bias in general-population and selected-sample treatment effects. *American Journal of Epidemiology*, kwae145., June 2024. ISSN 1476-6256. doi: 10.1093/aje/kwae145.
  48. Cecilia Maria Patino and Juliana Carvalho Ferreira. Internal and external validity: can you apply research study results to your patients? *Jornal Brasileiro de Pneumologia*, 44(3):183, May 2018. doi: 10.1590/S1806-37562018000000164.
  49. Irina Degtiar and Sherri Rose. A Review of Generalizability and Transportability. *Annual Review of Statistics and Its Application*, 10(1):501–524, March 2023. ISSN 2326-8298. doi: 10.1146/annurev-statistics-042522-103837.
  50. F. Godenschweger, U. Kägebein, D. Stucht, U. Yarach, A. Sciarra, R. Yakupov, F. Lüsebrink, P. Schulze, and O. Speck. Motion correction in MRI of the brain. *Physics in medicine and biology*, 61(5):R32, March 2016. doi: 10.1088/0031-9155/61/5/R32.
  51. Koene R. A. Van Dijk, Mert R. Sabuncu, and Randy L. Buckner. The influence of head motion on intrinsic functional connectivity MRI. *NeuroImage*, 59(1):431–438, January 2012. ISSN 1095-9572. doi: 10.1016/j.neuroimage.2011.07.044.
  52. Theodore D. Satterthwaite, Daniel H. Wolf, James Loughhead, Kosha Ruparel, Mark A. Elliott, Hakon Hakonarson, Ruben C. Gur, and Raquel E. Gur. Impact of in-scanner head motion on multiple measures of functional connectivity: relevance for studies of neurodevelopment in youth. *NeuroImage*, 60(1):623–632, March 2012. ISSN 1095-9572. doi: 10.1016/j.neuroimage.2011.12.063.
  53. Jonathan D Power, Kelly A Barnes, Abraham Z Snyder, Bradley L Schlaggar, and Steven E Petersen. Spurious but systematic correlations in functional connectivity MRI networks arise from subject motion. *NeuroImage*, 59(3):2142–2154, 2012.
  54. Benjamin E Yerys, Kathryn F Jankowski, Devon Shook, Lisa R Rosenberger, Kelly Anne Barnes, Madison M Berl, Eva K Ritzl, John Vanmeter, Chandan J Vaidya, and William Davis Gaillard. The fmri success rate of children and adolescents: typical development, epilepsy, attention deficit/hyperactivity disorder, and autism spectrum disorders. *Human brain mapping*, 30(10):3426–3435, 2009.
  55. K. J. Friston, S. Williams, R. Howard, R. S. Frackowiak, and R. Turner. Movement-related effects in fMRI time-series. *Magnetic Resonance in Medicine*, 35(3):346–355, March 1996. ISSN 0740-3194. doi: 10.1002/mrm.1910350312.
  56. Rastko Ciric, Adon F. G. Rosen, Guray Erus, Matthew Cieslak, Azeez Adebimpe, Philip A. Cook, Danielle S. Bassett, Christos Davatzikos, Daniel H. Wolf, and Theodore D. Satterthwaite. Mitigating head motion artifact in functional connectivity MRI. *Nature Protocols*, 13:2801–2826, December 2018. ISSN 1750-2799. doi: 10.1038/s41596-018-0065-y.
  57. Jonathan D. Power, Bradley L. Schlaggar, and Steven E. Petersen. Recent progress and outstanding issues in motion correction in resting state fMRI. *NeuroImage*, 0:536, January 2015. doi: 10.1016/j.neuroimage.2014.10.044.
  58. Jonathan D. Power. A simple but useful way to assess fMRI scan qualities. *NeuroImage*, 154:150–158., July 2017. ISSN 1095-9572. doi: 10.1016/j.neuroimage.2016.08.009.
  59. Theodore D. Satterthwaite, Mark A. Elliott, Raphael T. Gerraty, Kosha Ruparel, James Loughhead, Monica E. Calkins, Simon B. Eickhoff, Hakon Hakonarson, Ruben C. Gur, Raquel E. Gur, and Daniel H. Wolf. An improved framework for confound regression and filtering for control of motion artifact in the preprocessing of resting-state functional connectivity data. *NeuroImage*, 64:240–256, January 2013. ISSN 1053-8119. doi: 10.1016/j.neuroimage.2012.08.052.
  60. Max M. Owens, Nicholas Allgaier, Sage Hahn, DeKang Yuan, Matthew Albaugh, Shana Adise, Bader Chaarani, Joseph Ortigara, Anthony Juliano, Alexandra Potter, and Hugh Garavan. Multi-method investigation of the neurobiological basis of ADHD symptomatology in children aged 9-10:

- baseline data from the ABCD study. *Translational Psychiatry*, 11(64):1–11, January 2021. ISSN 2158-3188. doi: 10.1038/s41398-020-01192-8.
61. Mary Beth Nebel, Daniel E. Lidstone, Liwei Wang, David Benkeser, Stewart H. Mostofsky, and Benjamin B. Risk. Accounting for motion in resting-state fMRI: What part of the spectrum are we characterizing in autism spectrum disorder? *NeuroImage*, 257:119296., August 2022. ISSN 1095-9572. doi: 10.1016/j.neuroimage.2022.119296.
  62. Jonathan D. Power, Kelly Anne Barnes, Abraham Z. Snyder, Bradley L. Schlaggar, and Steven E. Petersen. Steps toward optimizing motion artifact removal in functional connectivity MRI; a reply to Carp. *NeuroImage*, 76:439–441, August 2013. ISSN 1053-8119. doi: 10.1016/j.neuroimage.2012.03.017.
  63. Joseph Biederman, Maura DiSalvo, Carrie Vaudreuil, Janet Wozniak, Mai Uchida, K. Yvonne Woodworth, Allison Green, Abigail Farrell, and Stephen V. Faraone. The Child Behavior Checklist Can Aid in Characterizing Suspected Comorbid Psychopathology in Clinically Referred Youth with ADHD. *Journal of psychiatric research*, 138:477, June 2021. doi: 10.1016/j.jpsychires.2021.04.028.
  64. Jae-won Kim, Ki-hong Park, Keun-ah Cheon, Boong-nyun Kim, Soo-churl Cho, and Kang-E. Michael Hong. The child behavior checklist together with the ADHD rating scale can diagnose ADHD in Korean community-based samples. *Canadian Journal of Psychiatry. Revue Canadienne De Psychiatrie*, 50(12):802–805, October 2005. ISSN 0706-7437. doi: 10.1177/070674370505001210.
  65. Kelly T. Cosgrove, Timothy J. McDermott, Evan J. White, Matthew W. Mosconi, Wesley K. Thompson, Martin P. Paulus, Carlos Cardenas-Iniguez, and Robin L. Aupperle. Limits to the generalizability of resting-state functional magnetic resonance imaging studies of youth: An examination of ABCD Study® baseline data. *Brain imaging and behavior*, 16(4):1919, August 2022. doi: 10.1007/s11682-022-00665-2.
  66. Ronald A Fisher. On the interpretation of  $\chi^2$  from contingency tables, and the calculation of p. *Journal of the Royal Statistical Society*, 85(1):87–94, 1922.
  67. Henry B Mann and Donald R Whitney. On a test of whether one of two random variables is stochastically larger than the other. *The annals of mathematical statistics*, pages 50–60, 1947.
  68. Frank Wilcoxon. Individual comparisons by ranking methods. *Biometrics bulletin*, 1(6):80–83, 1945.
  69. Brian MacMahon, Stella Yen, Dimitrios Trichopoulos, Kenneth Warren, and George Nardi. Coffee and cancer of the pancreas. *New England Journal of Medicine*, 304(11):630–633, 1981.
  70. Federica Turati, Carlotta Galeone, Valeria Edefonti, Monica Ferraroni, Pagona Lagiou, Carlo La Vecchia, and Alessandra Tavani. A meta-analysis of coffee consumption and pancreatic cancer. *Annals of oncology*, 23(2):311–318, 2012.
  71. Tyler J. VanderWeele and Miguel A. Hernán. Results on differential and dependent measurement error of the exposure and the outcome using signed directed acyclic graphs. *American Journal of Epidemiology*, 175(12):1303–1310, June 2012. ISSN 1476-6256. doi: 10.1093/aje/kwr458.
  72. María Jiménez-Buedo and Luis Miller. Why a Trade-Off? The Relationship between the External and Internal Validity of Experiments. *Theoria: Revista de teoría, historia y fundamentos de la ciencia*, ISSN 0495-4548, Vol. 25, N° 69, 2010, pags. 301-321, 25, September 2010. doi: 10.1387/theoria.779.
  73. Francesco Guala and Luigi Mittone. Experiments in economics: External validity and the robustness of phenomena. *Journal of Economic Methodology*, December 2005. URL <https://www.tandfonline.com/doi/abs/10.1080/13501780500342906>.
  74. Thomas D Cook and Donald T Campbell. *Quasi-experimentation: Design and analysis issues for field settings*. Houghton Mifflin, Boston, 1979.
  75. Donald T. Campbell. Experiments in social science: Their logic and conduct. *Handbook of*

Industrial and Organizational Psychology, 1963.

76. William R Shadish, Thomas D Cook, and Donald T Campbell. Experimental and quasi-experimental designs for generalized causal inference. Houghton Mifflin, Boston, 2002. ISBN 0-395-61556-9.
77. Drew H. Bailey, Alexander J. Jung, Adriene M. Beltz, Markus I. Eronen, Christian Gische, Ellen L. Hamaker, Konrad P. Kording, Catherine Lebel, Martin A. Lindquist, Julia Moeller, Adeel Razi, Julia M. Rohrer, Baobao Zhang, and Kou Murayama. Causal inference on human behaviour. Nature Human Behaviour, 8:1448–1459, August 2024. ISSN 2397-3374. doi: 10.1038/s41562-024-01939-z.
78. Shan H. Siddiqi, Konrad P. Kording, Josef Parvizi, and Michael D. Fox. Causal mapping of human brain function. Nature reviews. Neuroscience, 23(6):361, June 2022. doi: 10.1038/s41583-022-00583-8.
79. Lauren N. Ross and Dani S. Bassett. Causation in neuroscience: keeping mechanism meaningful. Nature Reviews Neuroscience, 25:81–90, February 2024. ISSN 1471-0048. doi: 10.1038/s41583-023-00778-7.
80. Peng Ding and Tyler J VanderWeele. Adjustment for collider bias in observational studies: a case study of effect of kidney function on mortality. Journal of the Royal Statistical Society: Series A (Statistics in Society), 178(4):915–930, 2015.
81. Hailey R. Banack and Jay S. Kaufman. Does selection bias explain the obesity paradox among individuals with cardiovascular disease? Annals of Epidemiology, 25(5):342–349, May 2015. ISSN 1873-2585. doi: 10.1016/j.annepidem.2015.02.008.
82. Raymond J Carroll, David Ruppert, and Leonard A Stefanski. Measurement error in nonlinear models. Chapman and Hall/CRC Monographs on Statistics and Applied Probability, 1995.
83. Saskia le Cessie, Jan Debeij, Frits R. Rosendaal, Suzanne C. Cannegieter, and Jan P. Vandembroucke. Quantification of Bias in Direct Effects Estimates Due to Different Types of Measurement Error in the Mediator. Epidemiology, 23(4):551, July 2012. ISSN 1044-3983. doi: 10.1097/EDE.0b013e318254f5de.
84. Miguel A. Hernán and James M. Robins. Estimating causal effects from epidemiological data. Journal of Epidemiology and Community Health, 60(7):578, July 2006. doi: 10.1136/jech.2004.029496.
85. Judea Pearl. Causality: Models, Reasoning and Inference. Cambridge University Press, Cambridge, England, UK, September 2009. doi: 10.5555/1642718.
86. Miguel A. Hernán and James M. Robins. Causal Inference: What If. Chapman & Hall/CRC, Boca Raton, 2020. ISBN 9781420076165.
87. W. G. Cochran. The Effectiveness of Adjustment by Subclassification in Removing Bias in Observational Studies, June 1968. URL <https://www.jstor.org/stable/2528036>. [Online; accessed 20. Feb. 2024].
88. Brian K. Lee, Justin Lessler, and Elizabeth A. Stuart. Weight Trimming and Propensity Score Weighting. PLoS ONE, 6(3), 2011. doi: 10.1371/journal.pone.0018174.
89. Michael J. Lopez and Roe Gutman. Estimation of Causal Effects with Multiple Treatments: A Review and New Ideas. Statistical Science, 32(3):432–454, August 2017. ISSN 0883-4237. doi: 10.1214/17-STS612.
90. Peter C. Austin. An Introduction to Propensity Score Methods for Reducing the Effects of Confounding in Observational Studies. Multivariate Behavioral Research, 46(3):399, May 2011. doi: 10.1080/00273171.2011.568786.
91. Paul R Rosenbaum and Donald B Rubin. Reducing Bias in Observational Studies Using Subclassification on the Propensity Score, September 1984. URL <https://www.jstor.org/stable/2288398>. [Online; accessed 20. Feb. 2024].
92. Nicholas C. Chesnaye, Vianda S. Stel, Giovanni Tripepi, Friedo W. Dekker, Edouard L. Fu,

- Carmine Zoccali, and Kitty J. Jager. An introduction to inverse probability of treatment weighting in observational research. *Clinical Kidney Journal*, 15(1):14, January 2022. doi: 10.1093/ckj/sfab158.
93. Daniel E. Ho, Kosuke Imai, Gary King, and Elizabeth A. Stuart. Matching as Nonparametric Pre-processing for Reducing Model Dependence in Parametric Causal Inference. *Political Analysis*, 15(3):199–236, July 2007. ISSN 1047-1987. doi: 10.1093/pan/mpl013.
  94. Donald B Rubin and Neal Thomas. Combining propensity score matching with additional adjustments for prognostic covariates. *Journal of the American Statistical Association*, 95(450): 573–585, 2000.
  95. Victoria Allan, Sreeram V. Ramagopalan, Jack Mardekian, Aaron Jenkins, Xiaoyan Li, Xianying Pan, and Xuemei Luo. Propensity score matching and inverse probability of treatment weighting to address confounding by indication in comparative effectiveness research of oral anticoagulants. *Journal of Comparative Effectiveness Research*, 9(9):603–614, June 2020. ISSN 2042-6313. doi: 10.2217/cer-2020-0013.
  96. Erinn M. Hade and Bo Lu. Bias associated with using the estimated propensity score as a regression covariate. *Statistics in medicine*, 33(1):74, January 2014. doi: 10.1002/sim.5884.
  97. Fan Li, Laine E. Thomas, and Fan Li. Addressing Extreme Propensity Scores via the Overlap Weights. *American Journal of Epidemiology*, 188(1):250–257, January 2019. ISSN 1476-6256. doi: 10.1093/aje/kwy201.
  98. Gary King, Richard Nielsen, Carter Coberley, James E. Pope, and Aaron Wells. Comparative Effectiveness of Matching Methods for Causal Inference, 2011. URL <https://gking.harvard.edu/publications/comparative-Effectiveness-Matching-Methods-Causal-Inference>. [Online; accessed 20. Feb. 2024].
  99. Gary King and Richard Nielsen. Why propensity scores should not be used for matching. *Political Analysis*, 27(4):435–454, 2019. URL <https://doi.org/10.1017/pan.2019.11>.
  100. Xing S Gu and Paul R Rosenbaum. Comparison of Multivariate Matching Methods: Structures, Distances, and Algorithms, December 1993. URL <https://www.jstor.org/stable/1390693>. [Online; accessed 20. Feb. 2024].
  101. Saad Jbabdi, Stamatios N. Sotiropoulos, Suzanne N. Haber, David C. Van Essen, and Timothy E. Behrens. Measuring macroscopic brain connections in vivo. *Nature Neuroscience*, 18:1546–1555, November 2015. ISSN 1546-1726. doi: 10.1038/nn.4134.
  102. Jinyong Hahn. On the Role of the Propensity Score in Efficient Semiparametric Estimation of Average Treatment Effects, March 1998. URL <https://www.jstor.org/stable/2998560>. [Online; accessed 20. Feb. 2024].
  103. James J Heckman and Edward Vytlacil. Structural Equations, Treatment Effects, and Econometric Policy Evaluation, May 2005. URL <https://www.jstor.org/stable/3598865>. [Online; accessed 20. Feb. 2024].
  104. R Core Team. *R: A Language and Environment for Statistical Computing*. R Foundation for Statistical Computing, Vienna, Austria, 2023. URL <https://www.R-project.org/>.
  105. James M Robins, Miguel Ángel Hernán, and Babette Brumback. Marginal structural models and causal inference in epidemiology. *Epidemiology*, 11(5):550–560, 2000.
  106. Thomas Lumley. *survey: Analysis of Complex Survey Samples*, 2023. URL <https://CRAN.R-project.org/package=survey>. R package version 4.2-1.
  107. Marius Hofert and Martin Mächler. Nested archimedean copulas meet R: The nacopula package. *Journal of Statistical Software*, 39(9):1–20, 2011. URL <https://www.jstatsoft.org/v39/i09/>.



**Appendix A. Methods for observational data (expanded).** To evaluate some of these methods, we consider  $n = 500$  samples from one of two batches (the exposures, in Figure 8(A)), where there are two covariates that are common causes (Figure 8.I). Samples with lower covariate values tend to more frequently receive the blue exposure, and samples with higher values tend to more frequently receive the orange exposure. In the upper-right and lower-left quadrants, in particular, note that the data illustrate violations of the positivity assumption: there are only points from one batch (and not the other) in these areas, indicating that individuals with these characteristics would likely not have been measured in the other batches.

**A.1 Inferring relationships through multivariate analyses** Confounding is typically addressed through a multivariate analysis. A *multivariate analysis* is a strategy in which we learn about the relationship between the exposure, the outcome, and other variables. The most direct approach is to employ a multiple regression model [17], where the outcome is modeled as a function of the exposure and a set of selected covariates (the *outcome model*). The core ID assumptions are that the conditional ignorability and positivity assumptions hold for the covariates included in the outcome model. When these ID assumptions are met, multiple regression models can identify a causal estimand. To achieve the further aim of a consistent estimate of the true causal effect typically requires assuming that the outcome model form is correct.

For instance, for our batch effects example, a common strategy is to regress the Measurement onto Batch and other demographic variables (such as Age and Sex) and discard additive and multiplicative biases in the Measurements or the error terms due to the Batch. Conceptually, the core aim is to remove the batch effect, while preserving the demographic effects in the subsequent data. This observation serves as inspiration for strategies such as ComBat [11] or ComBat-seq [18]. Multivariate regressions can often be powerful tools that facilitate the identification of causal estimands when appropriate models are leveraged.

Unfortunately, like unadjusted bivariate procedures, many multivariate procedures such as multiple regressions can be inadequate for yielding useful downstream insights. This materializes in practice through the related ideas of a lack of transparency about violations of the underlying ID assumptions and model misspecification bias. Regression models allow insights across the exposure groups through *extrapolation*: the estimation of effects for different combinations of the exposure and the covariates that may not exist in the observed data. In practice, regressions assume proper specification of the outcome model, and extrapolate based on the outcome model form, while ignoring violations of the positivity assumption (a source of the endogeneity issue) in all but extreme cases. This means that regression models can make opaque violations of a key ID assumption for the resulting regression to facilitate the estimation of causal effects, and subsequent conclusions become heavily dependent on the researcher-specified model form.

For instance, consider an attempt to correct a batch effect between Batch and Measurement, given demographic factors (e.g., Age and Biological Sex). If the two datasets have overlapping age ranges (e.g., between 10 and 80), and each have at least one member of each sex, a naive regression of Measurement onto Batch, Age, and Biological Sex will produce an estimate of a batch effect. However, perhaps in one batch all of the women are between the ages of 10 and 20, and in the other all of the women are between the ages of 20 and 80. This may constitute a violation of the positivity assumption, even though the regression will produce an answer and make opaque this violation. In less extreme cases, even if the positivity assumption and conditional ignorability for the included covariates are reasonable, a misspecified parametric outcome model form coupled with covariate imbalances can yield substantial estimation errors. In these cases, the analysis will hinge on the precision of the specified outcome model which, in most batch effect investigations, is unknown. Even if one's aims are not explicitly causal, attempting to understand phenomena without addressing endogeneity therefore may not produce scientifically useful conclusions, because the results may not actually reflect underlying

causal processes as a result of violations of the ID assumptions or model misspecifications for multiple regressions.

Some strategies directly attempt to make transparent violations of certain ID assumptions. These approaches employ techniques where, under certain ID assumptions, the endogeneity of the exposure given the covariates becomes irrelevant for subsequent inference [84]. In observational studies, these positivity-aware techniques can be viewed as methods that, under fairly general assumptions, may reduce potential sources of confounding biases in subsequent conclusions [85, 86]. Causal estimators aim to remove this bias by adjusting for common causes, effectively isolating the causal pathway of interest. With additional mechanistic assumptions, this reduction in bias may also enable mechanistic causal conclusions, even without direct experimental manipulation of mechanisms [84].

Conclusions drawn from these techniques may not necessarily involve actual mechanism manipulation when dealing with observational data. Therefore, deriving direct causal conclusions still requires somewhat stringent ID assumptions. Nonetheless, these techniques' ability to address many potential sources of bias makes them extremely valuable for scientific inquiry, even in the absence of mechanistic assumptions.

**A.2 Stratified methods** Stratification (or subclassification) is the most fundamental such technique. In a *stratified analysis*, common cause variables are partitioned into bins (called *strata*), allowing examination of the exposure-outcome relationship within each stratum [20, 21]. The underlying ID assumptions for stratified methods are that with sufficiently chosen bins, the exposures may be approximately ignorable and the positivity assumption may hold within each stratum. These stratum-specific effects can then be aggregated to estimate overall causal effects [23]. In this fashion, stratified methods have similar ID assumptions to more traditional non-stratified methods, but with the ID assumptions applied instead within-strata rather than over the entire covariate space. Additional assumptions for consistent estimation of causal effects typically include that the outcome model is approximately correctly specified within each stratum.

Compared to multivariate regression approaches, stratification with well-chosen bins can offer enhanced robustness, flexibility, and bias reduction [87]. In cases where the outcome model is misspecified globally, stratified regressions can offer non-parametric estimation where perhaps the outcome model may be more precise locally within-stratum, potentially reducing dependence on the specified model form as-compared to non-stratified multiple regression approaches. Further, stratified regressions can make more transparent violations of the ID assumptions, as one can directly investigate sparse or empty strata for particular exposure/covariate combinations. This yields direct insights into when certain techniques would instead be required to turn to extrapolation due to a lack of data support, and therefore informs when estimation may suffer. However, these methods also suffer from limitations: determining reasonable covariate bins may prove challenging in high-dimensional or complicated data structures (curse of dimensionality) [22], small sample sizes within individual bins may reduce estimation precision [23], and stratified methods may be sensitive to the specific sets of bins used (e.g., specific cut-points chosen to bin a continuous covariate) [22].

**A.3 Re-weighted methods** Other approaches, known as *re-weighted methods*, adjust the importance of different data points to make observational studies more like randomized experiments by rendering the exposure exogenous-like. This is done by assigning higher weights to some samples and lower weights to others [23]. Seminal re-weighted methods observed that in randomized experiments, samples with similar covariates will have an equal chance (the *propensity score*) of ending up in the exposure group versus the control. Under certain assumptions, these propensity scores encode *all* of the information about the covariates as they relate to the relationship between the exposure and the outcome. Re-weighting methods try to recreate this balance in observational data by making the propensity score distributions similar across exposure groups (called *adjustments*). In our batch effects example, such an adjustment would aim to make the exposure (the batch) appear more random and

exogenous-like, as it would be in a controlled experiment. Figure 8.II illustrates the propensity scores in our simulations.

**A.3.1 Propensity trimming** The simplest of these is known as *propensity trimming* (PT), which discards samples with propensity scores that are highly dissimilar from those in other exposure groups. This process reduces the number of samples with extreme propensities in both groups (Figure 8(B.II)). Since propensity scores encapsulate covariate information, PT also removes samples with atypical covariate profiles (Figure 8(B.I)), which could otherwise bias subsequent analyses [88]. This technique aims to achieve *covariate overlap*, a condition where individuals with similar characteristics could plausibly be observed in any exposure group, mimicking a randomized experiment. PT is typically leveraged in combination with other methods, such as regressions and other sequential causal techniques, as a data pre-processing step to enforce positivity onto the observed samples, and are rarely considered as standalone methods for estimating causal effects. The selection of samples for retention or removal can be done through various methods, including algorithmic approaches like vector matching (VM [89]). Another simple re-weighted method is *propensity stratification*, in which stratification is performed on the propensity scores instead of the covariates [90, 91].

**A.3.2 Inverse probability weighting** *Inverse probability weighting* (IPW) is another key re-weighting strategy. In IPW, samples are assigned weights inversely proportional to their propensity scores, typically estimated using logistic regression or multinomial models [23]. These weights are then used in subsequent analyses (e.g., a weighted regression) to approximately align the propensity distributions across exposure groups [24, 92]. In practice, IPW up-weights rare combinations of exposure and propensity. For instance, samples with high propensities in the orange group and low propensities in the blue group are given greater weight (Figure 8(C.II)). This process indirectly balances covariate distributions (Figure 8(C.I)) due to the relationship between covariates and propensity scores. When data features covariate distributions which are approximately equal, we say that the covariates are *covariate balanced* [23]. Various approaches exist for constructing these weights, with the choice depending on the specific inferential objectives [92]. ID assumptions for naive IPW methods are typically similar to other analytical approaches, including conditional ignorability and positivity, and consistent estimation requires an additional assumption that the propensity score model is correctly specified. This may appear to be no better than multiple regressions requiring correct specification of the outcome model. However, an advantage of IPW methods is that the construction of the propensity model can also give insights into the ID assumptions, in that a propensity score model with inflated or deflated influences of particular covariates can indicate violations of the positivity or conditional ignorability assumptions with respect to certain adjustment variables. The fit propensity model therefore can provide transparency for both ID and modeling assumptions jointly, required for resulting conclusions to be reasonable. However, this dependence on the propensity model has given rise to so-called *doubly robust* methods, where IPW methods are used in conjunction with multiple regressions (e.g., AIPW [25] or TMLE [26]). In these specifications, consistent estimates causal effects can be achieved if either the propensity score model or the outcome model are properly specified, allowing increased robustness for estimators to violations of model specifications.

**A.3.3 Matching methods** *Matching methods* are a more direct approach to achieve covariate balance. It approximates a “case-control” design by pairing samples (“matching” samples) from different exposure groups based on *covariate similarity*, which is typically estimated through a distance metric defined for the covariates. Samples without suitable matches are discarded from analysis [27]. We demonstrate this using propensity trimming followed by Mahalanobis distance-matching (Figure 8(D)). Matching methods are non-parametric and aim to equalize both marginal and joint covariate distributions across exposure groups [29] (Figure 8(D.I)). Due to the relationship between covariates and propensity scores, this also balances propensity score distributions (Figure 8(D.II)). Conceptually,

matching without replacement can be viewed as an extreme form of re-weighting: discarded samples receive a weight of 0, while matched samples receive a weight of 1 [23]. In a randomized experiment samples are affixed a probability for each exposure group (potentially dependent on covariates); for a given set of covariates, there will be exposed and unexposed individuals at a relatively constant rate so long as the sample size is large enough. Intuitively, matching methods mimic this observation, by explicitly enforcing that there are similar exposed and unexposed individuals for a given set of covariates. A closely related variation is known as *propensity matching*, in which matching is performed on the propensity scores instead of the covariates [23].

Subsequent techniques can be applied to the samples leveraging the sample weights from a re-weighted analysis. These methods can often be complementary; a popular strategy is to first perform propensity trimming, then use a re-weighting technique such as matching (Figure 8(C, D)), and finally a multiple regression approach for the ultimate inference task. While these methods can offer substantial improvements in the bias of subsequent estimators [93, 94], it is important to clarify that they are not truly doubly robust, due to the fact that the steps are combined sequentially rather than simultaneously like traditional doubly robust methods, so failures of either the outcome model or the matching can yield biases in subsequent analyses.

**A.3.4 Limitations of techniques that address exposure endogeneity** Re-weighted methods address many issues but have their own limitations. Propensity score methods summarize covariates into a single score, allowing analysis of all individuals [95]. However, they are sensitive to model selection bias, especially with poor covariate overlap [96], and many weighted propensity score methods (such as IPW) require subsequent analytical tools be chosen which are compatible with weights. Additionally, higher-weighted units dominate results, effectively reducing sample size [97]. Distance-based matching methods can offer greater flexibility and efficiency than propensity-based approaches [98, 99]. They also tend to be simpler for augmenting existing analyses as there are no requirements that subsequent procedures incorporate weights. Yet, they require careful selection of distance metrics and covariate pre-processing. Their performance also degrades with high-dimensional covariates (curse of dimensionality) [23, 100]. An important general limitation of all these methods is their reliance on measuring relevant common causes, or sufficiently general subsets of them. The challenge of unobserved confounding persists and is discussed further in Section 2.2. The advantages and limitations of the methods described herein are summarized in Table 1.

## Appendix B. Definitions.

1. *variables*: the characteristics that will be analyzed, as well as other extraneous factors that effect these characteristics.
2. *causal mechanism*: cause-and-effect relationships of one variable on another, encoded by arrows. For example,  $E \rightarrow Y$  encodes that  $E$  causes  $Y$ .
3. *exposure*: variable at the base of an edge in a causal graph, “the cause”, typically denoted by  $E$ .
4. *outcome*: variable at the head of an edge in a causal graph, “the affected variable”, typically denoted by  $Y$ .
5. *estimand of interest*: the relationship between two variables that one wishes to estimate.
6. *estimator*: rule for computing a desired effect from observed data.
7. *identification (ID) assumptions*: the assumptions under which conclusions about the causal effect of the exposure on the outcome can be drawn using the observed data.
8. *unadjusted bivariate analysis*: the process of deriving conclusions about the relationship between an exposure and an outcome by looking only at how the outcome changes as a function of the exposure.
9. *statistical consistency*: a property of estimators in which estimates become more precise for an estimand of interest with more data.

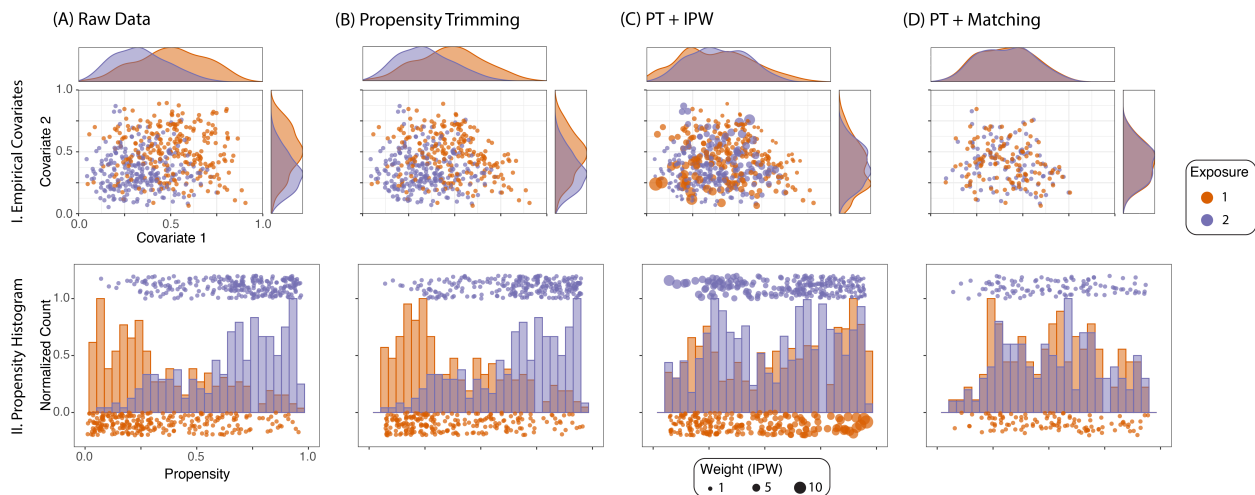


Figure 8: **A conceptual illustration of approaches to adjust for confounding biases.** (A).I  $n = 500$  samples are drawn from two possible exposures with equal probability, where covariate distributions differ based on the exposure. (A).II illustrates the estimated propensity scores from logistic regression, as histograms. (B) Propensity trimming tends to exclude samples which are radically dissimilar across the exposure groups. This has the effect of filtering samples with extreme values in terms of the covariates in (B.I), and the propensity scores in (B.II), and “overlaps” the empirical distributions of the covariates. (C) Re-weighting approaches (where point size indicates weights) leverage weights so that the propensity distributions (after re-weighting) are approximately equal across the exposure groups. (C.I) weighted covariate distributions and weighted marginal distributions tend to be approximately equal, and (C.II) the weighted histograms tend to be approximately similar across the exposures. (D) matching methods tend to yield approximately equal covariate distributions across the groups, and the covariates are “balanced”. This is illustrated by the retained samples having nearly equal distributions for the covariates in (D.I) and the propensities in (D.II).

10. *bias*: the tendency of an estimator to systematically mis-estimate an underlying estimand of interest.
11. *exogenous variable*: a variable whose value is imposed on the system by the assignment mechanism.
12. *endogenous variable*: a variable whose values change in response to changes in other variables in the system.
13. *causal path*: alternating sequences of variables and relationships (indicated by arrows), where we can follow relationships from one variable to the next.
14. *direct effect*: the effect of one variable on another without other variables intervening; e.g., if  $E \rightarrow Y$  and  $E \rightarrow M \rightarrow Y$ , the direct effect is the effect  $E \rightarrow Y$ .
15. *indirect effect*: the effect of one variable on another mediated by other variables; e.g., if  $E \rightarrow Y$  and  $E \rightarrow M \rightarrow Y$ , the indirect effect is the effect  $E \rightarrow M \rightarrow Y$ .
16. *ancestor*: variables upstream on a causal path with respect to another variable; e.g., if  $X_1 \rightarrow Y \rightarrow X_2$ ,  $X_1$  is an ancestor of  $Y$  and  $X_2$ .
17. *descendant*: variables downstream on a causal path with respect to another variable; e.g., if  $X_1 \rightarrow Y \rightarrow X_2$ ,  $X_2$  is a descendant of  $X_1$  and  $Y$ .
18. *total effect*: the cumulative effect of all possible pathways through which the exposure could influence the outcome
19. *causal mediation analysis*: a strategy that attempts to attribute effects of an exposure on an outcome to either direct effects (exposure on the outcome) or indirect effects (exposure on other variables on the outcome).
20. *backdoor path*: a path that starts with an arrow pointing into the exposure and ends with a relationship pointing into or out of the outcome; e.g., for an exposure  $E$  and outcome  $Y$ , the path  $E \leftarrow X \rightarrow Y$ .



21. *common cause*: a variable that affects both the exposure and the outcome; often referred to as a confounder; e.g., for an exposure  $E$  and outcome  $Y$ ,  $X$  is a common cause if  $E \leftarrow X \rightarrow Y$ . Stated another way, common causes are ancestors of the exposure and the outcome.
22. *confounding bias*: spurious, non-causal variability which arises between an exposure and an outcome.
23. *conditional ignorability*: an ID assumption which asserts that all factors that affect both the exposures and the outcomes can be captured by the observed covariates; also known as “no unmeasured confounding”.
24. *positivity*: an ID assumption which asserts that any given individual could plausibly have received either exposure level, based on their individual characteristics.
25. *exposure consistency*: an ID assumption which asserts that the each possible exposure corresponds to a single, well-defined intervention that could be obtained for a given individual (the *potential outcomes*), and that the exposure actually received corresponds to the potential outcome for that exposure level.
26. *stable-unit treatment value assumption (SUTVA)*: an ID assumption that requires that exposures are independent, also known as “no interference”.
27. *blocking a path*: tailoring an analysis such that spurious non-causal variability due to certain variables is controlled for.
28. *sensitivity analysis*: analytical technique which attempts to investigate the degree to which uncertainty in the output of a model can be attributed to uncertainties in the model input. Sensitivity analyses are commonly used when investigating the robustness of causal methods to confounding biases due to different types of unobserved variables.
29. *collider*: a descendant of two or more variables in a causal graph; often referred to as a *common outcome*; e.g., if  $E$  is an exposure and  $Y$  is an outcome,  $C$  is a collider if  $E \rightarrow C \leftarrow Y$ .
30. *selection bias*: a bias which, loosely, occurs when the individuals selected for analysis can bias subsequent conclusions.
31. *internal bias*: a type of bias which arises when conditioning on a selection variable creates an unblocked non-causal path between the exposure and outcome.
32. *net-external bias*: a bias which occurs when how outcomes would respond to an exposure differs across these groups of individuals whose membership in the selected sample can be differently affected by the exposure.
33. *collider stratification bias*: a type of bias that arises in an investigation due to conditioning an analysis on a collider.
34. *measurement errors*: difference between a measured value and the true underlying value of a phenomena one wishes to capture.
35. *non-differential measurement error*: a measurement error in which both (i) the measured exposure is independent of the true outcome conditional on the true exposure, and (ii) the measured outcome is independent of the true exposure conditional on the true outcome.
36. *multivariate analysis*: a strategy in which we learn about the relationship between the exposure, the outcome, and other variables.
37. *extrapolation*: estimation of effects for different combinations of the exposure and the covariates that may not exist in the observed data.
38. *stratified analysis*: an analysis technique in which samples are divided into covariate bins (strata), and analyses are performed within each stratum and aggregated to derive global conclusions.
39. *re-weighted method*: an analysis technique in which the importance of particular samples are altered to make observational studies more like randomized experiments by rendering the exposure exogenous-like.

40. *propensity score*: a probability of receiving a particular exposure, given the covariates.
41. *propensity trimming (PT)*: a data pre-processing step common to many analysis techniques in which samples with unusually high or low propensities for certain exposures are discarded from subsequent analysis as a form of outlier removal.
42. *covariate overlap*: a condition where individuals with similar characteristics could plausibly be observed in any exposure group.
43. *inverse probability weighting (IPW)*: an analysis technique in which samples are assigned weights inversely proportional to their propensity scores, and then the weights are incorporated into subsequent analyses to approximately align the propensity distributions across exposure groups.
44. *covariate balance*: a condition where the joint covariate distributions are approximately equal across exposure groups.
45. *doubly robust method*: an analysis technique in which consistent estimates of causal effects can be achieved if either the propensity score or outcome model are properly specified.
46. *matching method*: an analytical technique which approximates a “case-control” design by pairing samples (“matching” samples) from different exposure groups based on *covariate similarity*, typically estimated through a distance metric defined for the covariates.

## Appendix C. Simulations.

**C.1 No Unobserved Common Cause Simulations** We turn to simulation to illustrate the effectiveness of control procedures for the estimation of causal effects in simulated diffusion connectome data, which are an extension of the procedures developed in [28].  $n = 200$  samples are assigned to one of two simulated exposures (batches, color), and then have a single covariate sampled for each individual. The covariate overlap quantifies the degree of covariate balance between the two batches; when the covariate balance is less than 1, individuals in the blue batch tend to have higher covariates than the orange batch. In these situations, the exposure is endogenous, and the covariates are confounding. In human diffusion connectomes, the edge-weight is the number of fibers bridging pairs of ROIs (edges are counts) [101]. Edge-weights are sampled, where the relationship between the covariate and the log of the number of fibers is non-linear but monotonic (Figure 9(A), the systematic component of a Poisson regression model). The “batch effect” is the difference between the expected log of the expected number of fibers for each of the two batches, here having a magnitude of 1. A standard measure of effect size in the causal literature is called the Conditional Average Treatment Effect (CATE) [102, 103], which is the difference in the expected number of fibers (for each age) at this edge that would have been observed had a particular individual been observed in the orange batch versus the blue batch (red band, Figure 9(B)).

The goal is to estimate and remove this “batch effect” from each sample, thereby “aligning” the data from each batch. Fit methods include parametric regression models (purple, bivariate poisson bivariate, conditional poisson conditional, and oracle poisson oracle), stratified methods (blue, propensity trimmed + stratified poisson stratified), and re-weighted methods (green, inverse probability-weighted poisson ipw and matching poisson matching, with each incorporating propensity trimming). conditional is closely related to the ComBat-seq procedure [18], which represents the gold standard literature approach for batch effect correction in count data (such as diffusion connectomes or read counts in genomics data). Only oracle knows the true underlying relationship between the covariates and the log of the number of fibers, and therefore serves as a lower-bound for all methods. Only the parametric regression models incorporate the covariates into the systematic component of the model. The remaining positivity-aware methods (stratified, ipw, matching) address only the endogeneity of the exposure, but do not actually use the covariates in the subsequent regression. Stated another way, these methods subvert estimating the covariate/outcome relationship entirely, instead only practically addressing exposure endogeneity.

We quantify the effectiveness of each strategy by assessing the estimation error across  $R = 1000$  trials between the estimated batch effect and the true batch effect ( $y$ -axis) for (i) when there is a batch effect between the samples of magnitude 1 (Figure 9(C)), and (ii) when there is no batch effect present, but batch effect correction is performed anyways (Figure 9(D)). As positivity-aware methods inherently reduce the sample size and the effective sample size, it is possible that reductions in bias for positivity-aware methods is offset by increases in variance of the estimates. Therefore, we assess all techniques using the average absolute difference between estimates and the underlying true batch effect, as approaches with low bias but high variance could see low estimation error if a non-absolute difference were employed. We repeat this for different levels of covariate balance ( $x$ -axis) between the two batches. As the outcomes are a function of the covariates, there are open backdoor paths when covariate overlap is less than 1.

Whenever covariate overlap is less than 1, non-positivity-aware methods are empirically dominated by the positivity-aware methods. In particular, `matching` achieves near the optimal performance of `oracle`, despite not using the covariates for the subsequent regression, and addressing the endogeneity of the exposure using only non-parametric distance methods. These conclusions are consistent across all regimes except for purely linear regimes, where the underlying assumptions of the linear models used are appropriate. Taken together, these results suggest that non-positivity-aware methods are subject to strong biases due to endogeneity of the exposure, and only achieve similar performance to positivity-aware methods in the limited setting when extrapolatory assumptions are appropriate. On the other hand, positivity-aware methods show greater levels of robustness to model misspecifications and endogeneities that may arise in the exposure. In essence, we have exchanged modest increases in variance (sample sizes and effective sample sizes are effectively reduced by positivity-aware methods) for far more performant estimands with much lower bias.

**C.1.1 Simulation Settings** For each  $i$ ,  $T_i \stackrel{iid}{\sim} \text{Bern}(0.5)$ .  $T_i$  denotes the group of each individual.

With  $u$  denoting “covariate unbalancedness”, let:

$$X_i \stackrel{iid}{\sim} \begin{cases} 2\text{Beta}(\alpha, \alpha u) - 1, T_i = 0 \\ 2\text{Beta}(\alpha u, \alpha) - 1, T_i = 1 \end{cases}$$

Stated another way, when  $u > 1$ , the covariate distributions (across groups) are asymmetric, and the covariate is associated with the grouping variable. “Covariate overlap” measures the similarity of the covariate distributions, conditional on the group; e.g.:

$$\text{overlap} = \int_{-1}^1 \min(f(x|T_i = 0), f(x|T_i = 1)) \, dx$$

If  $u = 1$ , that  $X_i|T_i = 0 \stackrel{\mathcal{D}}{=} X_i|T_i = 1$ , and  $\text{overlap} = 1$ . As  $u \rightarrow \infty$ , the covariates become less and less balanced, and  $\text{overlap} \rightarrow 0$ .

In general, for the  $k^{\text{th}}$  dimension, the outcome model is:

$$Y_{ik} \sim \text{Pois}(\lambda_{ik}), \quad \lambda_{ik} = \mathbb{E}[Y_{ik}]$$

The different settings denote different relationships for the mean model denoted by  $\lambda_{ik}$ , given below. The simulations are repeated with two outcome dimensions, and incorporate a scaling factor over each dimension such that the first dimension carries most of the covariate/outcome relationship.

*Linear*

$$\log(\lambda_{ik}) = \frac{1}{d_k} (2X_i - 1 + T_i)$$

There is a linear “covariate effect” between the covariate  $X_i$  and the log of the expected outcome (given by the Poisson rate parameter).

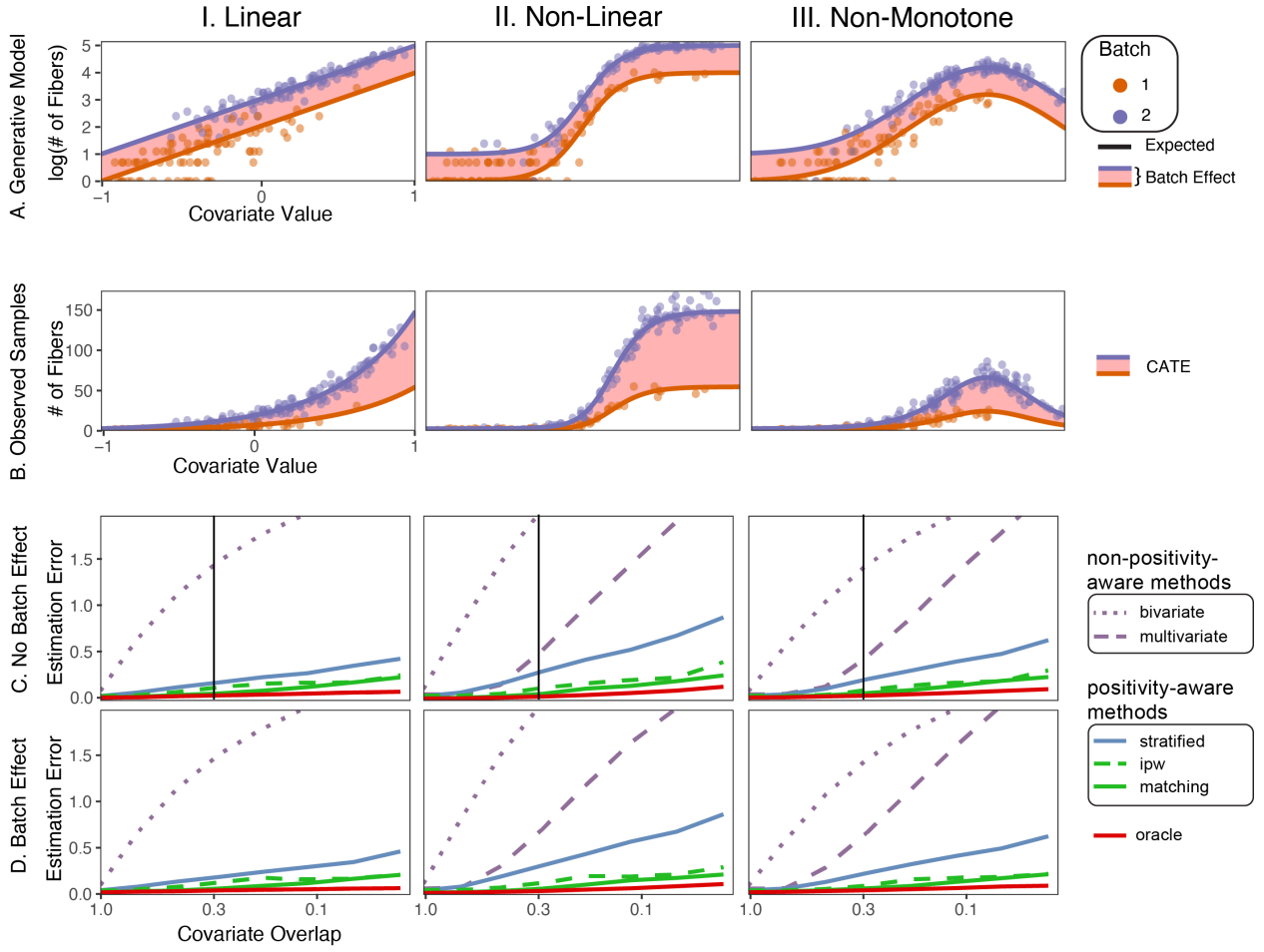


Figure 9: **Comparison of multivariate, stratified, and re-weighted methods for controlling confounding (Extended).** (A) shows the systematic component of the generative model for the count data. In this case, we model the log of the expected number of fibers (solid lines) for each batch as a linear, non-linear, or non-monotone function of the covariate value, with an offset (red) for the batch effect. Observed samples for a single trial are shown with circles. (B) shows the generative model on the response scale (e.g., after log-transforming). The CATE is the difference between the blue and orange lines. (C) shows the estimation error when no batch effect is present in the data generating model, and (D) shows the estimation error when a batch effect of magnitude 1 is present in the data generating model. The vertical bar in (C) delineates the covariate overlap setting for Appendix Figure 10(A). Simulation settings are detailed in Appendix C.1.1.

### Non-linear

$$\log(\lambda_{ik}) = \frac{1}{d_k} (4\text{sigmoid}(8X_i) + T_i)$$

where:

$$\text{sigmoid}(x) = \frac{1}{1 + \exp(-x)}$$

There is a non-linear “covariate effect” between the covariate  $X_i$  and the log of the expected outcome (given by the Poisson rate parameter). Under this scenario, the regression models across positivity-aware and non-positivity-aware methods are misspecified, though the relationship between the covariates and the outcome is still monotonic (minor misspecification).

### Non-monotone

$$\log(\lambda_{ik}) = \frac{1}{d_k} (4\phi(X_i, 0.5, 0.5) + T_i)$$

Where:

$$\phi(x, \mu, \sigma) = \frac{1}{\sigma\sqrt{2\pi}} \exp\left(-\frac{(x - \mu)^2}{2\sigma^2}\right)$$

is the pdf of the normal distribution with mean  $\mu$  and variance  $\sigma^2$ . There is a non-monotone ‘‘covariate effect’’ between the covariate  $X_i$  and the log of the expected outcome (given by the Poisson rate parameter). Under this scenario, the regression models across positivity-aware and non-positivity-aware methods are misspecified, in that the relationship is both non-linear and non-monotone.

### C.1.2 Confounding control methods

*bivariate* The bivariate model is a poisson regression model, where we model:

$$\log(\mathbb{E}[Y_i|t_i]) = \beta_T t_i + \beta_0$$

The bivariate model is implemented via `glm` package in R [104]. For all of the above settings, the bivariate model will not include the true data generating distribution.

*multivariate* The multivariate model is a poisson regression model, where we model:

$$\log(\mathbb{E}[Y_i|t_i, x_i]) = \beta_T t_i + \beta_X x_i + \beta_0$$

The multivariate model is implemented via `glm` package in R [104]. The multivariate model only includes the true data generating distribution for the linear setting.

*stratified* The stratified model is a poisson regression model that incorporates covariate stratification. We first divide the covariate space into  $n_{strata}$  equally spaced intervals. Then, we model:

$$\log(\mathbb{E}[Y_i|t_i, s_i]) = \beta_T t_i + \sum_{j=1}^{n_{strata}} \beta_{S_j} \mathbf{1}(s_i = j) + \beta_0$$

where  $s_i$  represents the stratum to which the  $i$ -th observation belongs, and  $\mathbf{1}(s_i = j)$  is an indicator function that equals 1 when observation  $i$  is in stratum  $j$ , and 0 otherwise. This formulation allows for a separate intercept for each stratum, effectively creating a step function over the covariate space. The stratified model is implemented using the `glm` function from the `stats` package in R [104], with the `strata` function used to create the stratification. This approach allows for a non-parametric adjustment of the covariate effect, potentially capturing non-linear relationships between the covariate and the outcome. The stratified model could approximate the true data generating distribution for non-linear and non-monotone relationships, depending on the number of strata used (we use 5 arbitrarily).

*ipw* We first perform propensity trimming with `vm`, an approach for removing samples with high/low propensities [89]. For nominal treatments, the generalized propensity score  $r(t, x)$  is the probability  $Pr(\mathbf{t} = t | \mathbf{x} = x)$  of being assigned to group  $t$  given the baseline covariates  $x$ . For a given individual with baseline covariates  $x_i$ , a set of generalized propensity scores  $\mathcal{R}(x_i) = \{\hat{r}(t, x_i)\}_{t \in [K]}$  are estimated using a multinomial regression model. For each group  $t \in [K]$ , we compute the following quantities:

$$(1) \quad l(t) \triangleq \max_{t' \in [K]} \left( \min_{i \in [n]: t_i = t'} \{\hat{r}(t, x_i)\} \right), \quad h(t) \triangleq \min_{t' \in [K]} \left( \max_{i \in [n]: t_i = t'} \{\hat{r}(t, x_i)\} \right)$$

Individuals  $i$  with  $\hat{r}(t, x_i) \notin (l(t), h(t))$  for any  $t \in [K]$  are discarded from successive hypothesis testing. Intuitively, `vm` ensures that no retained individuals have covariates which occur with extremely low probability (or extremely high probability) for any particular group.



Next, using logistic regression, we model:

$$\text{logit}(\mathbb{E}[T_i]) = \beta_\tau x_i$$

and we estimate probabilities of being assigned to group 1 (the propensities) with:

$$\hat{p}_i = \text{expit}(\beta_\tau x_i)$$

We use these estimated propensities to construct inverse probability weights:

$$w_i = \begin{cases} \frac{1}{\hat{p}_i}, & t_i = 1 \\ \frac{1}{1-\hat{p}_i}, & t_i = 0 \end{cases}$$

The intuition of inverse probability weighting is to create a pseudo-population where the treatment assignment is independent of the observed covariates [13, 105]. If treated units ( $t_i = 1$ ) look less likely to be treated ( $\mathbb{P}(T_i = 1; x_i)$  is small), we up-weight their importance to better represent similar individuals who didn't receive the treatment ( $t_i = 0$ ) but could have. If non-treated units ( $t_i = 0$ ) look more likely to be treated, we up-weighted their importance to better represent similar individuals who did receive treatment ( $t_i = 1$ ) but might not have [86].

We then use these weights to perform a weighted bivariate regression with `svyglm` from the package `survey` [106]. Like `bivariate`, the regression model itself does not include the true underlying data generating distribution.

*matching* We first perform propensity trimming with `vm`, described above.

Next, we perform Mahalanobis distance matching [23]. This process entails matching each treated individual (with  $t_i = 1$ ) to a control individual ( $t_i = 0$ ). Control individuals are selected based on the nearest neighbor approach, using the Mahalanobis distance as the metric of similarity across covariates. If no suitable control individual can be identified within 0.2 standard deviations (the caliper width) for each covariate, the treated individual is discarded from subsequent analysis. This procedure aims to balance the covariate distributions between the treated and control groups, reducing potential confounding effects. Matching is implemented with the `MatchIt` package [29].

We then use the “covariate balanced” sample to perform a bivariate regression, as-per `bivariate`. Like `bivariate`, the regression model itself does not include the true underlying data generating distribution.

*oracle* The oracle model is a poisson regression model, where the regression model utilized exactly matches the underlying covariate/outcome model. For the linear setting, this is:

$$\log(\lambda_{ik}) = \beta_X X_i + \beta_T T_i + \beta_0$$

For the non-linear setting:

$$\log(\lambda_{ik}) = \beta_X \text{sigmoid}(8X_i) + \beta_T T_i + \beta_0$$

and for the non-monotone setting:

$$\log(\lambda_{ik}) = \beta_X \phi(X_i, 0.5, 0.5) + \beta_T T_i + \beta_0$$

It is called an “oracle” because across all settings, the fit model leverages the underlying ground truth of the covariate/outcome relationship.

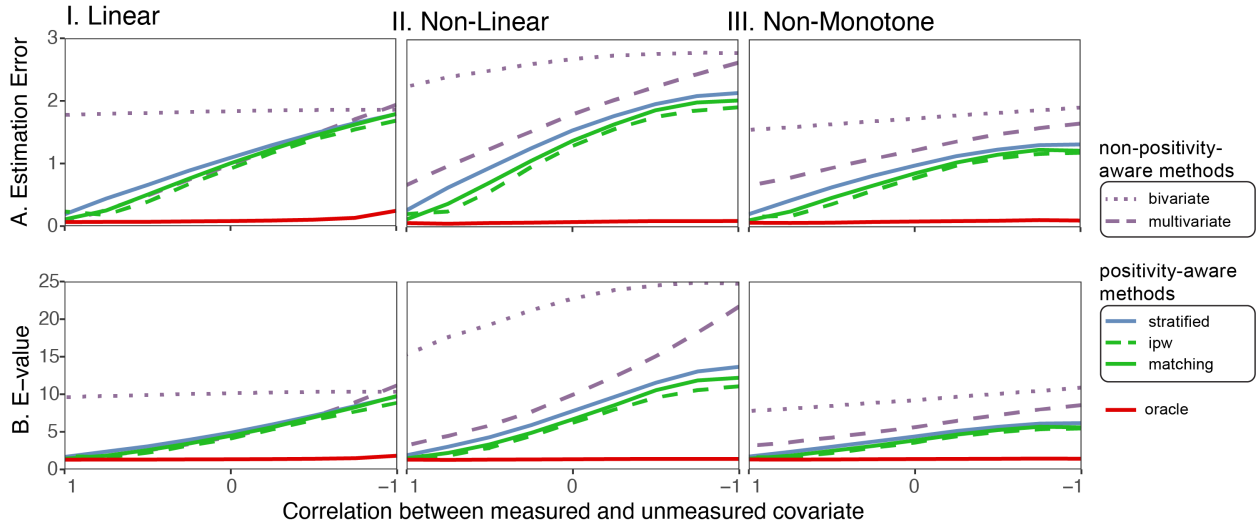


Figure 10: **Effect of unobserved confounding on the estimation of causal effects.** (A) adds an unobserved covariate which is related to the measured covariate by a correlation ( $x$ -axis) with covariate balance fixed around 0.3 (Figure 9(C), vertical bar). (B) the average e-values for each method for the experiments from (A). Simulation settings are detailed in Appendix C.2.

**C.2 Unobserved common cause simulations** Our simulations are augmented to include a second covariate which is unobserved (Figure 10(A)) for the case where no batch effect is present (analogous to Figure 9(C) at a measured covariate balance around 0.3). This unobserved covariate is chosen to make the treatment-outcome relationship appear greater than it actually is given the measured covariate when correlation is low or negative. All methods are performed by disregarding the unobserved covariate, except `oracle` which knows the true relationship between the unobserved covariate and the outcome. When this unobserved covariate is highly correlated with the measured covariate, all methods see similar performance to when no unobserved covariate was present.

We illustrate the average e-value across all trials for different values of the correlation (Figure 10(B)). Recall that as there is no treatment-outcome relationship (the true batch effect is 0), a small estimation error consists of the methods correctly identifying that there is no treatment-outcome relationship. All methods except `bivariate` see low e-values with high correlation between the measured and unobserved covariates in the linear regime (Figure 10(B.I)). No confounding is needed to “explain away” the treatment-outcome relationship, as the other methods correctly estimate no treatment-outcome relationship (and consequently, the e-value is low). Further, across all regimes, the e-value increases relatively monotonically for a given method as the correlation decreases. The unobserved covariate is more strongly associated with the treatment and the outcome given the measured covariate when the correlation is low or negative; the e-value correctly reflects this and is higher as correlation decreases.

When the model is misspecified (Figure 10(B.II+III)), `multivariate` misrepresents the treatment-outcome relationship even when correlation is high. Therefore, higher amounts of unobserved confounding would be needed to completely explain away the detected treatment-outcome relationship than for positivity-aware methods `stratified`, `ipw`, or `matching`. This illustrates a crucial feature of the e-value: while in isolation one may conclude that this illustrates that estimated treatment-outcome relationship by `multivariate` may be more robust to unobserved confounding than positivity-aware techniques (the e-values are higher across all experiments), the e-value makes no assumptions about the estimation accuracy of the method itself. Therefore, unsuitably chosen methods (such as `multivariate`) which do not facilitate precise estimation in the absence of unobserved confounding will have that imprecision “absorbed” into the e-value when unobserved confounding is present. Stated another way, there are multiple factors which explain the estimation error of `multivariate` ((i) model misspecifi-

ation for measured covariates and (ii) unobserved confounding), but the e-value attributes all of this estimation error to the unobserved confounding. This shows that sensitivity analyses must be performed holistically in light of analyses as to the estimation or testing precision of a given method in the absence of confounding (which we performed in Figure 9(C)).

**C.2.1 Simulation Settings** For  $i \in [n]$  where  $n = 200$ ,  $T_i \stackrel{iid}{\sim} \text{Bern}(0.5)$ .  $T_i$  denotes the group of each individual, and  $X_i$  denotes the covariate for the individual, as-above. The level of covariate overlap is fixed at around 0.3 (moderate covariate overlap across the groups).

We introduce the unobserved covariate  $U_i$ , where:

$$U_i \stackrel{iid}{\sim} \begin{cases} 2\text{Beta}(1, 3) - 1, T_i = 0 \\ 2\text{Beta}(3, 1) - 1, T_i = 1 \end{cases}$$

and:

$$\text{Corr}(U_i, X_i) = \rho$$

denotes the correlation between the observed and unobserved covariates. This introduces an additional covariate which may be more (or less) associated with the observed covariates. When  $\rho$  is closer to 1, it is possible that control for  $X_i$  may be sufficient to also control for  $U_i$ . When  $\rho$  is closer to 0 or negative, proper control for  $X_i$  may worsen control for  $U_i$ , introducing unobserved confounding biases to the analysis. Correlate covariates were generated with specified distributions using the `copula` package [107] via Gaussian copulas.

*Linear*

$$\log(\lambda_{ik}) = \frac{1}{d_k} (X_i + U_i - 1 + T_i)$$

There is a linear “covariate effect” between the covariate  $X_i$ , the unobserved variable  $U_i$ , and the log of the expected outcome (given by the Poisson rate parameter).

*Non-linear*

$$\log(\lambda_{ik}) = \frac{1}{d_k} (2\text{sigmoid}(8X_i) + 2\text{sigmoid}(8U_i) + T_i)$$

where:

$$\text{sigmoid}(x) = \frac{1}{1 + \exp(-x)}$$

There is a non-linear “covariate effect” between the covariate  $X_i$ , the unobserved variable  $U_i$ , and the log of the expected outcome (given by the Poisson rate parameter).

*Non-monotone*

$$\log(\lambda_{ik}) = \frac{1}{d_k} (2\phi(X_i, 0.5, 0.5) + 2\phi(U_i, 0.5, 0.5) + T_i)$$

Where:

$$\phi(x, \mu, \sigma) = \frac{1}{\sigma\sqrt{2\pi}} \exp\left(-\frac{(x - \mu)^2}{2\sigma^2}\right)$$

is the pdf of the normal distribution with mean  $\mu$  and variance  $\sigma^2$ . There is a non-monotone “covariate effect” between the covariate  $X_i$ , the unobserved variable  $U_i$ , and the log of the expected outcome (given by the Poisson rate parameter).

**C.2.2 Unobserved confounding control methods** We use the same control methods, except for `oracle`. The `oracle` method uses a poisson regression model, where the regression model utilized exactly matches the underlying covariate/outcome model (for both observed and unobserved covariates). For the linear setting, this is:

$$\log(\lambda_{ik}) = \beta_X X_i + \beta_U U_i + \beta_T T_i + \beta_0$$

For the non-linear setting:

$$\log(\lambda_{ik}) = \beta_X \text{sigmoid}(8X_i) + \beta_U \text{sigmoid}(8U_i) + \beta_T T_i + \beta_0$$

and for the non-monotone setting:

$$\log(\lambda_{ik}) = \beta_X \phi(X_i, 0.5, 0.5) + \beta_U \phi(U_i, 0.5, 0.5) + \beta_T T_i + \beta_0$$

**C.3 Collider Simulations** We generate simulations under the model noted in Figure 5(B). Measurements are offset from an underlying neurological property if they are low-motion (the offset is zero-mean noise) or high-motion (the offset has a positive mean, simulating the positive correlations induced by head motion).  $n = 200$  samples are generated with a demographic covariate (e.g., age) and a genetic risk for the behavioral phenotype of interest (e.g., ASD). The demographics and genetic risk influence the underlying neurology for a simulated individual, and together all three factors influence a sample’s likelihood to have the underlying behavioral phenotype via a logistic model (the outcome model). The relationship between the cumulative effects of demographics, genetic risk, and the underlying neurology with the outcome is either linear, non-linear, or non-monotone. The underlying neurology, behavioral phenotype, and demographic profile together influence the simulated head motion for an individual. If the head motion exceeds a given threshold, the measurements are corrupted by a differential measurement error; otherwise, the motion is zero-mean noise. The goal is to estimate the effect of the underlying neurology on the behavioral phenotype, only observing the underlying neurology through the corrupted measurements. `oracle` uses the true underlying measurements (with no differential measurement error) as well as the true underlying outcome model to address common-cause confounding biases, and serves as a benchmark for other strategies. `naive` estimates the effect of the measurements on the outcome (ignorant the differential measurement error) using logistic regression, `filtering` is similar to `naive` but first removes the high-motion samples.

Non-causal effects (functions of distribution of the exposure conditioned on the outcome) introduce the challenge in that it is difficult to produce benchmarks under a causal model, such as Figure 5(B), in that the estimand of interest for these approaches is not an underlying parameter for the model. To subvert this challenge, the simulations of [61] do not actually feature a differential measurement error (rather, only a collider) nor any form of confounding (despite including demographic covariates), which simplifies the problem of identifying the underlying spurious effect. An “optimal” strategy in their simulation context is to simply compare the means between the ASD phenotype and TD phenotype individuals, and ignore the collider all together (a reverse-causal `naive` strategy which ignores head motion). The asymptotic behavior of such a strategy serves as the gold standard for the simulations described. While their simulations illustrate that their proposed strategy `drtmle` outperforms a reverse-causal `filtering` approach when colliders are present in the absence of differential measurement errors and confounding, no comparisons are generated to the reverse-causal `naive` strategy in the smaller sample regimes where the reverse-causal `naive` strategy should be optimal, nor is there indication of the extent to which any of the techniques are performant for estimating the reverse effect when faced with differential measurement errors or confounding biases. We believe that our simulations amend these challenges. The underlying deconfounded group difference (the “true” reverse causal effect from [61]) is estimated by direct computation using the true underlying measurements

(with no differential measurement error) with a much greater sample size ( $N = 100,000$ ), and `drtmle` estimates the deconfounded group difference using the procedure described in [61].

We evaluate the performance of these techniques for estimating their underlying estimand in Figure 11(A) by examining the average absolute difference, analogous to that in Figure 9(C-D). No strategies perform particularly well in light of the `oracle` method, though `filtering` appears to be maximally similar to the `oracle`. When searching for brain-behavior relationships in neuroimaging data, a useful construction are statistical tests which investigate whether no underlying effect is present against the alternative that an effect is present. While `drtmle` is not estimating an underlying causal effect (a spurious effect, as-described above) and does not see particularly high performance in terms of estimation error, it is possible that its simplification of the problem to a deconfounded group difference is useful for statistical testing.

Figure 11(B) investigates the sensitivity of these tests to changes in the underlying effect size ( $\alpha = 0.05$ , black dotted line). As the effect size increases, sensitive tests will tend to reject the null hypothesis at a higher rate, and therefore see an increase in statistical power. `naive` is the only test which is sensitive. `drtmle` and `filtering` reach high power only for the extreme values of effect size, and also see a non-monotonic relationship between effect size and power. This can indicate that these strategies may be conflating non-veridical effects with the underlying causal effect, and non-veridical effects may be obfuscating the underlying causal effect. Figure 11(C) investigates the specificity of these tests when no underlying effect is present. As confounding increases, non-specific tests may alias confounding biases with the the underlying causal effect, leading to more false discoveries (type I statistical errors) even though no true causal effect is present; specific tests will tend to make type I errors at a rate of approximately  $\alpha = 0.05$  (black dotted line). None of the methods are particularly specific, and tend to make type I errors at rates in excess of five-fold higher than one would expect.

**C.3.1 Simulation Settings** For  $i \in [n]$  where  $n = 200$ , we generate an unobserved confounder conveying genetic risk for the outcome (e.g., ASD) as  $R_i \stackrel{iid}{\sim} \text{Bern}(0.25)$ . Independently, we generate an observed covariate (e.g., measured intelligence) related to the neuroimaging measurement and the outcome. The underlying true biological property (e.g., true underlying neurology) is:

$$T_i \sim \begin{cases} 2\text{Beta}(4(1 + 0.2X_i), 2) - 1, & R_i = 1 \\ 2\text{Beta}(4(1 + 0.2X_i), 4(1 + 0.2X_i)) - 1, & R_i = 0 \end{cases}$$

Both the unobserved confounder and the observed covariate alter the distribution of the underlying true biological property. The risk for the outcome is:

$$\mathbb{P}(Y_i = 1) = \text{expit}(\eta T_i + f(X_i) - 1.5)$$

where  $\eta$  is the “effect size” (the estimand of interest; e.g., the degree to which  $T_i$  causes the outcome  $Y_i$ ), and  $f(X_i)$  is a function of the covariates. The unobserved confounder (e.g., genetic risk for the outcome) influences the outcome through the underlying true biological property. Further, in-line with existing beliefs regarding ASD/ADHD, risk for the outcome is heightened when the underlying true biological property takes higher values (e.g., ASD/ADHD are caused by heightened brain connectivity).

Next, we generate a random variable corresponding to whether a sample is high motion ( $U_i = 1$ ):

$$\mathbb{P}(U_i = 1) = 1 - \text{expit}(T_i + 2X_i + 2Y_i - 1.5).$$

For a given covariate level, individuals with the outcome and/or individuals with larger values of the true underlying biological property typically have high motion data. Finally, the observed measurements are biased due to motion artifacts:

$$T_i^* = 0.8T_i + 0.2 \begin{cases} 2\text{Beta}(10, 2) - 1, & U_i = 1 \\ 2\text{Beta}(10, 10) - 1, & U_i = 0 \end{cases}$$



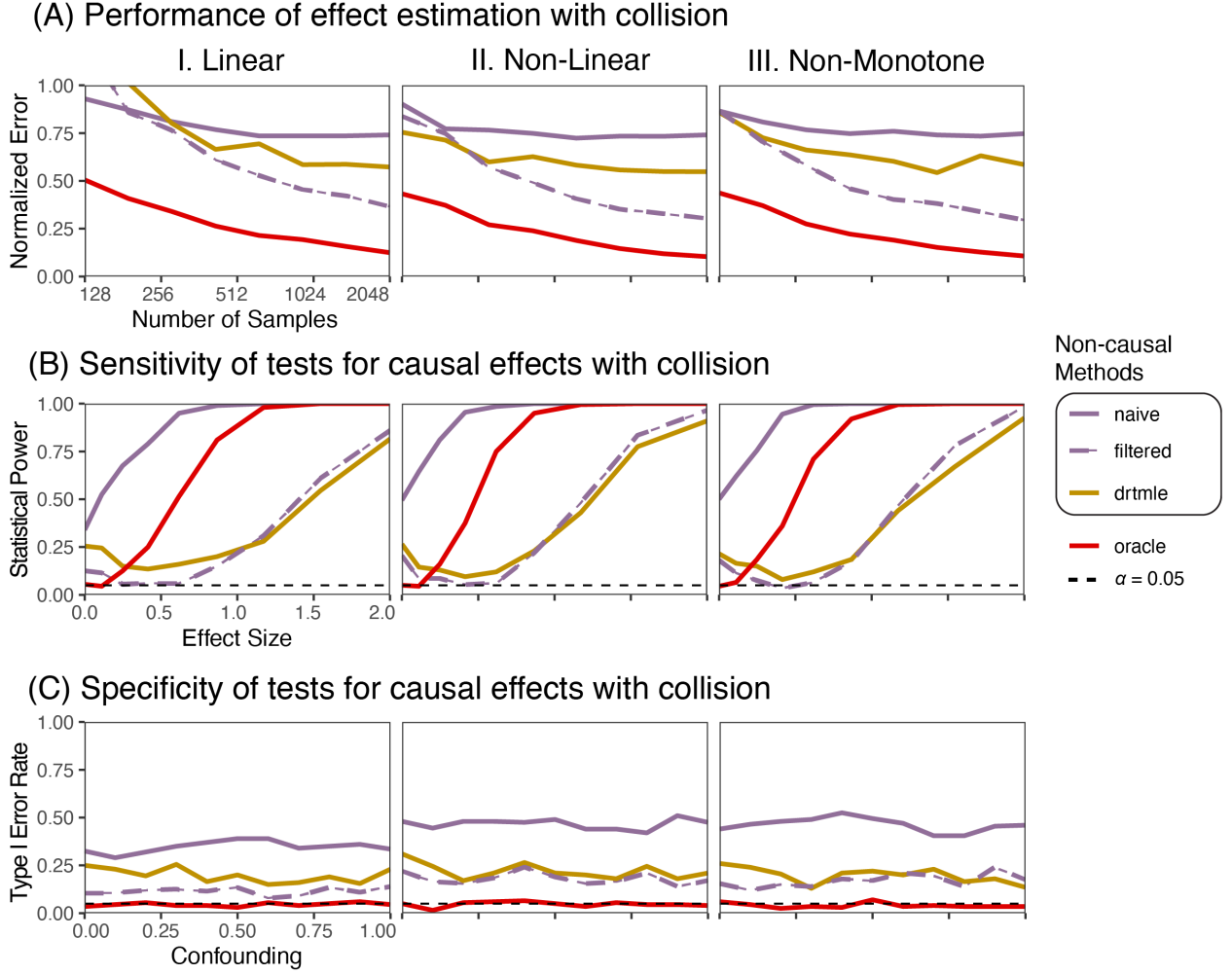


Figure 11: **Comparison of positivity-aware and non-positivity-aware methods for addressing challenge posed by head motion.** (A) comparison of methods for estimating causal effects with collision and confounding.  $x$ -axis denotes sample size, and  $y$ -axis denotes the normalized estimator error, which is the normalized difference between the estimated effect and the underlying true causal effect (all methods except `drtmle`, which instead estimates the deconfounded group difference). Positivity-aware methods show higher performance than non-positivity-aware methods. (B) + (C) tests whether an estimated causal effect is significant. (B) investigates test sensitivity, where sensitive tests are tests which see higher statistical power as the underlying effect size increases. `naive` methods show similar sensitivity to `oracle` methods. (C) investigates test specificity, where specific tests have a type two rate approximately equivalent to the alpha of the tests ( $\alpha = 0.05$ , dashed black line), as a function of the level of confounding of the true causal relationship ( $x$ -axis). `matching` is the only specific test.

When the data is high-motion ( $U_i = 1$ ),  $T_i^*$  is a weighted combination of the underlying biological measurement, and positively-skewed error term (e.g., the observed measurements will be “overly correlated”). When the data is low-motion ( $U_i = 0$ ),  $T_i^*$  is a weighted combination of the underlying biological measurement, and zero-mean error.

We repeat this across three regimes, denoting the relationship between the observed confounder and the outcome:

- *Linear*:  $f(X_i) = 2X_i$ .
- *Non-Linear*:  $f(X_i) = 2\text{sigmoid}(2X_i)$ .
- *Non-Monotone*:  $f(X_i) = 2\phi(X_i, 0.5, 0.5)$ .

### C.3.2 Methods

*naive* The naive model directly performs a logistic regression of  $Y_i$  onto the observed measurements and the covariates. The model is:

$$\text{logit}(\mathbb{E}[Y_i; t_i^*, x_i]) = \beta_T t_i^* + \beta_X x_i + \beta_0,$$

and our estimate of  $\eta$  is  $\hat{\beta}_T$ . The naive model is implemented via `glm` package in R [104].

*filtered* The filtered model directly performs a logistic regression of  $Y_i$  onto the observed measurements and the covariates. The model is:

$$\text{logit}(\mathbb{E}[Y_i; t_i^*, x_i]) = \beta_T t_i^* + \beta_X x_i + \beta_0,$$

for  $i$  where  $u_i = 0$ . Points are ignored if they are high-motion ( $u_i = 1$ ). Our estimate of  $\eta$  is  $\hat{\beta}_T$ . The filtered model is implemented via `glm` package in R [104].

*drtmle* `drtmle` is implemented using an adaptation of the code provided by Nebel et al. [61].

`drtmle` does not investigate a causal relationship between the the cause ( $T_i$ , as-measured by  $T_i^*$ ) and the outcome ( $Y_i$ ); rather, `drtmle` investigates a reverse causal relationship between the outcome and the cause. The estimand of interest for `drtmle` is the “deconfounded group difference”, defined as:

$$\psi = \mathbb{E}[\mathbb{E}[T_i^* | Y_i = 1, U_i = 0, X_i] | Y_i = 1] - \mathbb{E}[\mathbb{E}[T_i^* | Y_i = 0, U_i = 0, X_i] | Y_i = 0]$$

If  $U_i = 0$ , then  $T_i^* = 0.8T_i + Z_i$  where  $Z_i$  is a zero-mean error term (the data is “usable”). Therefore, as  $\mathbb{E}[T_i^* | U_i = 0, Y_i, X_i] = 0.8\mathbb{E}[T_i | Y_i, X_i]$  because  $\mathbb{E}[Z_i | U_i = 0, X_i, Y_i] = 0$ , the deconfounded group difference is equivalent to:

$$\psi = 0.8 (\mathbb{E}[\mathbb{E}[T_i | Y_i = 1, X_i] | Y_i = 1] - \mathbb{E}[\mathbb{E}[T_i | Y_i = 0, X_i] | Y_i = 0])$$

This quantity can be estimated from the data by direct computation from the underlying true biological property  $T_i$  and their corresponding outcomes  $Y_i$ . As-per Nebel et al. [61], we estimate the true deconfounded group difference using 100,000 samples from the same data-generating distribution as the simulation setting. Since `drtmle` is not estimating a causal effect, for the purposes of investigating the normalized error of `drtmle`, we instead compare the estimates of `drtmle` to estimates of  $\psi$ , as-per above.

*Oracle* The oracle knows both the unobserved (true) measurements and the relationship between the covariates  $X_i$  and the outcomes  $Y_i$ , and uses the logistic regression model:

$$\text{logit}(\mathbb{E}[Y_i]) = \beta_T T_i + \beta_X f(X_i) + \beta_0,$$

The estimate of  $\eta$  is  $\hat{\beta}_T$ . The oracle model is implemented via `glm` package in R [104].

#### Appendix D. ABCD Exploratory Analysis.

We first test for demographic differences across the sites in the ABCD study. Data were amalgamated using the files and corresponding key in `participants_v1.0.3.zip`, retrieved from [https://nda.nih.gov/edit\\_o](https://nda.nih.gov/edit_o) [31]. To test whether the distribution of covariates differs across sites, we turn to the following hypothesis tests:

$H_0$  : the covariate distributions are the same across all sites

$H_A$  : the covariate distributions differ between at least two sites  $k$  and  $l$

For continuous or ordinal covariates, we use the Kruskal-Wallis (KW) test, a non-parametric  $K$ -sample test, analogous to a  $K$ -way ANOVA, which can be used to test whether the distribution of

Demographic Covariate	Covariate type	Test	adjusted $p$ -value
Percent right-handed	binary	FFH	< 0.001
Percent with anaesthesia exposure	binary	FFH	< 0.001
Parental income group	ordinal (> 2 levels)	KW	< 0.001
Parental education level	ordinal (> 2 levels)	KW	< 0.001
Learning/memory PC	continuous	KW	< 0.001
Executive function PC	continuous	KW	< 0.001
General ability PC	continuous	KW	< 0.001
Age	continuous	KW	< 0.001
Percent Latinx	binary	FFH	< 0.001
Percent Asian	binary	FFH	< 0.001
Percent black	binary	FFH	< 0.001
Percent white	binary	FFH	< 0.001
Percent parent-identified as male	binary	FFH	0.826

Table 2: Tests and outcomes for each covariate, across sites in the ABCD study.

a continuous or ordinal predictor differs across the  $K$  groups [34]. For binary covariates, we use the Fisher-Freeman-Halton (FFH) test, a non-parametric test which can be used to test whether the probability of a given predictor (i.e., the binary covariate) differs across a particular exposure (i.e., one-of- $K$  sites). This test approximates the exact distribution of the contingency table using Monte Carlo methods [33]. The outcomes of the statistical tests are delineated in Table 2.

Next, we group the demographic covariate information across groups based on the level of average motion from volume-to-volume in the resting state fMRI scan, using the real-time motion tracking information for the resting state fMRI sessions. This was performed by combining the preceding demographic information with the real-time motion tracking information for the resting state fMRI sessions found in the file `abcd-data-release-5.0.zip`, in the expanded file `core/imaging/mri_y_qc_motion.csv`, from the homepage for the ABCD study (non-imaging raw data, June 2023, from <https://nda.nih.gov>). The relevant columns corresponding to the real-time motion tracking information for the resting state fMRI sessions are `rsfmri_meanmotion`, “Resting state fMRI - Average framewise displacement in mm”, and `rsfmri_subthreshnvol`, “Resting state fMRI - Number of frames with FD < 0.2”. We also annotate the raw scores for the CBCL found in the file `abcd-data-release-5.0.zip`, in the expanded file `core/mental_health/mh_p_cbcl.csv`. The relevant columns corresponding to the raw and T scores for ADHD were `cbcl_scr_dsm5_adhd_r` and `cbcl_scr_dsm5_adhd_t`, corresponding to “Recommended ADHD CBCL DSM5 Scale (raw score)” and “Recommended ADHD CBCL DSM5 Scale ( $t$  score)” respectively. The keys for the motion and CBCL data to identify the appropriate columns were retrieved by filtering through <https://data-dict.abcdstudy.org/>. Data are grouped based on whether the mean FD across all volumes exceeds (exclusion group) or is less than (inclusion group) 0.5.

To test whether the distribution of demographic covariates and CBCL data differ across the excluded (mean FD  $\geq 0.5$ ) or included (mean FD < 0.5) samples, we test:

$H_0$  : the covariate distributions are the same between the groups

$H_A$  : the covariate distributions differ between the two groups

For continuous or ordinal covariates, we use the Mann-Whitney-Wilcoxon  $U$  test, a non-parametric 2-sample test, analogous to a 2-way ANOVA, which can be used to test whether the distribution of a continuous or ordinal predictor differs between two groups [67, 68]. For binary covariates, we use the Fisher exact (FE) test, a non-parametric test which can be used to test whether the probability of a given predictor (i.e., the binary covariate) differs across a particular exposure (i.e., one-of- $K$  sites). This test

Demographic Covariate	Covariate type	Test	adjusted $p$ -value
ADHD CBCL DSM5 Scale	ordinal (> 2 levels)	$U$	< 0.001
Percent right-handed	binary	FE	< 0.001
Percent with anaesthesia exposure	binary	FE	0.501
Parental income group	ordinal (> 2 levels)	$U$	< 0.001
Parental education level	ordinal (> 2 levels)	$U$	< 0.001
Learning/memory PC	continuous	$U$	< 0.001
Executive function PC	continuous	$U$	< 0.001
General ability PC	continuous	$U$	< 0.001
Age	continuous	$U$	< 0.001
Percent Latinx	binary	FE	0.109
Percent Asian	binary	FE	1.000
Percent black	binary	FE	< 0.001
Percent white	binary	FE	< 0.001
Percent parent-identified as male	binary	FE	< 0.001

Table 3: Tests and outcomes for each covariate, across sites in the ABCD study.

is an exact test, and intuitively tests how extreme a given contingency table is using the properties of a contingency table with the hypergeometric distribution [66]. The outcomes of the statistical tests are delineated in Table 3.